Check for updates

A Novel Mechanism, Linked to Cell Density, Largely Controls Cell Division in *Synechocystis*[1][OPEN]

Alberto A. Esteves-Ferreira,[a,b] Masami Inaba,[a] Toshihiro Obata,[c] Antoine Fort,[d] Gerard T.A. Fleming,[e] Wagner L. Araújo,[f] Alisdair R. Fernie,[c] and Ronan Sulpice[a,2]

[a]National University of Ireland-Galway, Plant Systems Biology Laboratory, Plant and AgriBiosciences Research Centre, School of Natural Sciences, Galway, Ireland
[b]CAPES Foundation, Ministry of Education of Brazil, Brasilia DF 70040 020, Brazil
[c]Central Metabolism Laboratory, Department of Molecular Physiology, Max Planck Institute of Molecular Plant Physiology, Max Planck Society, 14476 Potsdam-Golm, Germany
[d]National University of Ireland-Galway, Genetics and Biotechnology Research Laboratory, Plant and AgriBiosciences Research Centre, School of Natural Sciences, Galway, Ireland
[e]National University of Ireland-Galway, Microbiology, School of Natural Sciences, Galway, Ireland
[f]Max-Planck Partner Group at the Departamento de Biologia Vegetal, Universidade Federal de Viçosa, 36570-900 Vicosa, Minas Gerais, Brazil

ORCID IDs: 0000-0001-7618-4748 (M.I.); 0000-0001-8931-7722 (T.O.); 0000-0002-6113-9570 (R.S.).

Many studies have investigated the various genetic and environmental factors regulating cyanobacterial growth. Here, we investigated the growth and metabolism of *Synechocystis* sp. PCC 6803 under different nitrogen sources, light intensities, and CO_2 concentrations. Cells grown on urea showed the highest growth rates. However, for all conditions tested, the daily growth rates in batch cultures decreased steadily over time, and stationary phase was obtained with similar cell densities. Unexpectedly, metabolic and physiological analyses showed that growth rates during log phase were not controlled primarily by the availability of photoassimilates. Further physiological investigations indicated that nutrient limitation, quorum sensing, light quality, and light intensity (self-shading) were not the main factors responsible for the decrease in the growth rate and the onset of the stationary phase. Moreover, cell division rates in fed-batch cultures were positively correlated with the dilution rates. Hence, not only light, CO_2, and nutrients can affect growth but also a cell-cell interaction. Accordingly, we propose that cell-cell interaction may be a factor responsible for the gradual decrease of growth rates in batch cultures during log phase, culminating with the onset of stationary phase.

Cyanobacteria were the first organisms on Earth that performed oxygenic photosynthesis, and nowadays, they are widespread on a variety of terrestrial and aquatic habitats, showing extensive metabolic, physiological, and morphological diversity (Tomitani et al., 2006; Beck et al., 2012; Schirrmeister et al., 2013). This diversity among cyanobacteria has been related to their ability to adapt to a series of changes that occurred on Earth, affecting the availability of atmospheric oxygen, light, CO_2, and reduced nitrogen (Catling et al., 2001; Herrero et al., 2001; Kasting and Siefert, 2002; Kühl et al., 2005; Muramatsu and Hihara, 2012; Hagemann et al., 2016).

Synechocystis sp. PCC 6803 (hereafter termed *Synechocystis*) is one of the cyanobacterial species commonly used for metabolic and genetic studies. It is easy to culture under phototrophic, mixotrophic, and heterotrophic conditions, its entire genome is sequenced, and it exhibits natural competence for the incorporation of exogenous DNA (Kanesaki et al., 2012; Yu et al., 2013). Like all photosynthetic organisms, the physiology and cell cycle of *Synechocystis* are affected by both light availability and intensity (Yang et al., 2010; Schuurmans et al., 2015). Light harvesting is performed by phycobilisomes composed of a core of allophycocyanins and branches of phycocyanin (Mullineaux, 2008; Arteni et al., 2009). The light energy is transferred from the phycobilisomes to chlorophyll *a* present in the reaction centers of PSI and PSII (Liu et al., 2013). These

[1] A.A.E-F. is recipient of scholarships granted by the Agency for the Support and Evaluation of Graduate Education (CAPES-Brazil; grant no. BEX 8904/13-8) and the Thomas Crawford Hayes (National University of Ireland-Galway). R.S. is the recipient of a Visiting Professor grant from CNPq-Brazil (PVPE grant no. 401090/2014-0) and the Millennium Fund (National University of Ireland-Galway).

[2] Address correspondence to ronan.sulpice@nuigalway.ie.

The author responsible for distribution of materials integral to the findings presented in this article in accordance with the policy described in the Instructions for Authors (www.plantphysiol.org) is: Ronan Sulpice (ronan.sulpice@nuigalway.ie).

A.A.E.-F. and R.S. conceived the original research plans; A.A.E.-F. and T.O. performed most of the experiments; M.I., A.F., and G.T.A.F. provided technical assistance and helped in the design of experiments; A.A.E.-F. and R.S. designed the experiments and analyzed the data; A.A.E.-F. and R.S. conceived the project and wrote the article with contributions of all the authors; A.R.F., G.T.A.F., and W.L.A. supervised and complemented the writing.

[OPEN] Articles can be viewed without a subscription.

www.plantphysiol.org/cgi/doi/10.1104/pp.17.00729

 © 2017 American Society of Plant Biologists. All Rights Reserved.
Downloaded from on August 30, 2017 - Published by www.plantphysiol.org
Copyright © 2017 American Society of Plant Biologists. All rights reserved.

transfers lead to the generation of reducing power, which supply metabolic processes such as the Calvin-Benson cycle and nitrogen uptake and reduction (Valladares et al., 2002; Flores et al., 2005). The efficiency of CO_2 fixation and assimilation is, at least partially, under the control of a carbon concentration mechanism, which increases the CO_2 concentration around the Rubisco catalytic site (Price et al., 1998), allowing it to operate close to its V_{max} (Badger et al., 2006). *Synechocystis* can take up and metabolize different nitrogen sources (nitrate, nitrite, ammonium, urea, and some amino acids; Quintero et al., 2000; Valladares et al., 2002; Flores et al., 2005; Muro-Pastor et al., 2005). Intriguingly, the control of the expression and activity of transporters and enzymes related to nitrogen metabolism is regulated by a complex network involving 2-oxoglutarate, NtcA (nitrogen control factor of cyanobacteria), PII (nitrogen regulatory protein PII), and PipX (PII-interacting protein X; Alfonso et al., 2001; Herrero et al., 2001; Llácer et al., 2010; Zhao et al., 2010; Espinosa et al., 2014; Lüddecke and Forchhammer, 2015).

In photobioreactors, *Synechocystis* can typically achieve growth rates ranging from 1.7 to 2.5 divisions per day (i.e. doubling times of between 14.1 and 9.6 h; Kim et al., 2011). Faster doubling times of 6 and 5.6 h were reported by Hihara et al. (2001) and Zavřel et al. (2015), respectively; however, in the case of the latter study, these division rates could not be maintained for more 120 h. Many studies have attempted to identify growth-limiting factors in *Synechocystis* (e.g. nutrients and light; Kim et al., 2011; Lea-Smith et al., 2014; Burnap, 2015; Touloupakis et al., 2015; van Alphen and Hellingwerf, 2015). Understanding of the factors controlling the limitation of *Synechocystis* growth would facilitate the use of this strain as a cell factory (Yu et al., 2013) for the production of biomass (Joseph et al., 2014), pigments (Sekar and Chandramohan, 2008), secondary metabolite natural products (Frommeyer et al., 2016), biofuel (Dexter and Fu, 2009; Baebprasert et al., 2011; Liu et al., 2011), and other high-value compounds.

The commercialization of cyanobacteria-based biomass and biomolecules still requires optimization for sustainable economic viability (Schenk et al., 2008; Brennan and Owende, 2010; Wijffels et al., 2013). One recently adopted approach in this view is the use of low-cost sources of CO_2, nutrients, and water (Markou and Georgakakis, 2011; Slade and Bauen, 2013; Iijima et al., 2015). In this study, we grew *Synechocystis* in various growth conditions, using three different nitrogen sources, in combination with two light intensities and two CO_2 concentrations. Urea is seemingly a potent source of nitrogen supporting the growth of *Synechocystis*, as it promoted high cell division rates and is less costly than nitrate and ammonium. That said, after 4 d of culture, growth was inhibited for all conditions tested, and this inhibition was not related to a metabolic limitation. Indeed, we observed an uncoupling of photosynthesis and growth, leading to the accumulation of unused reserves in the cells and even their release to culture medium. We further investigated the reasons behind this nonmetabolic growth limitation and conclude that nutrient limitation and quorum sensing are not responsible for the decrease of growth rates during the log phase and for the onset of the stationary phase. Our data also suggest that self-shading is not responsible for the growth limitation. We hypothesize that *Synechocystis* may be able to sense the gradual increase of cell density occurring in batch cultures via cell-cell interaction, leading to the gradual decrease of division rate until the onset of stationary phase.

RESULTS

Rates of Cell Division Peak at the Start of Log Phase and Then Decrease Gradually

The growth cycle and generation time (Gt) of *Synechocystis* varied in response to the nitrogen source, light intensity, and CO_2 concentration (Fig. 1; Table I). A lag phase was not observed when cells were grown in the presence of ammonium under moderate light intensity (ML; 50 μmol photons m^{-2} s^{-1}), nitrate under ML with CO_2 supplementation, and nitrate under high light intensity (HL; 200 μmol photons m^{-2} s^{-1}; Fig. 1, A–D). The highest number of divisions per day was typically achieved at day 2 or 3 and decreased gradually afterward (Fig. 1, B, D, and F). The cultures reached a stable stationary phase after 8 to 14 d (Fig. 1). Curiously, the stationary phase occurred at similar cell densities (2.1 to 2.6 $\times$ 10^8; Fig. 1; Supplemental Table S1), despite a large variation in the duration of the growth cycles, in nine out of the 10 growth conditions studied. In order to confirm whether cells were in stationary phase, we analyzed the expression of the *ftsZ* (cell division protein FtsZ) gene, which encodes the cell division protein FtsZ (Supplemental Fig. S1). The relative *ftsZ* expression levels of the cells at stationary phase, at the end of the day (ED), were 4 to 10 times lower than the levels observed for cells in log phase (Supplemental Fig. S1A). In addition, as observed previously (Mori and Johnson, 2001), the *ftsZ* expression levels were very low at the end of the night (EN), with little differences between the growth stages (Supplemental Fig. S1B), thus confirming that cells do not divide at night.

The gradual decrease in the number of divisions per day observed from the 3rd or 4th day of culture and the fact that cultures reached stationary phase with comparable cell densities regardless of differences in nitrogen source, light intensity, and CO_2 concentration raised questions about a similar metabolic limitation occurring for all these growth conditions due to (1) nutrient starvation, (2) reduction in light intensity or quality due to high cell density (self-shading), or (3) a regulatory limitation of growth due to quorum sensing. In order to test these hypotheses, we analyzed the photosynthetic rates and cellular metabolic contents and evaluated the possibilities of nutrient depletion, quorum sensing, and self-shading.

Metabolic and Physiological Traits during the Log Phase

The varied growth conditions did not affect *Synechocystis* cell size (Supplemental Table S2). Then, as our

Downloaded from on August 30, 2017 - Published by www.plantphysiol.org
Copyright © 2017 American Society of Plant Biologists. All rights reserved.

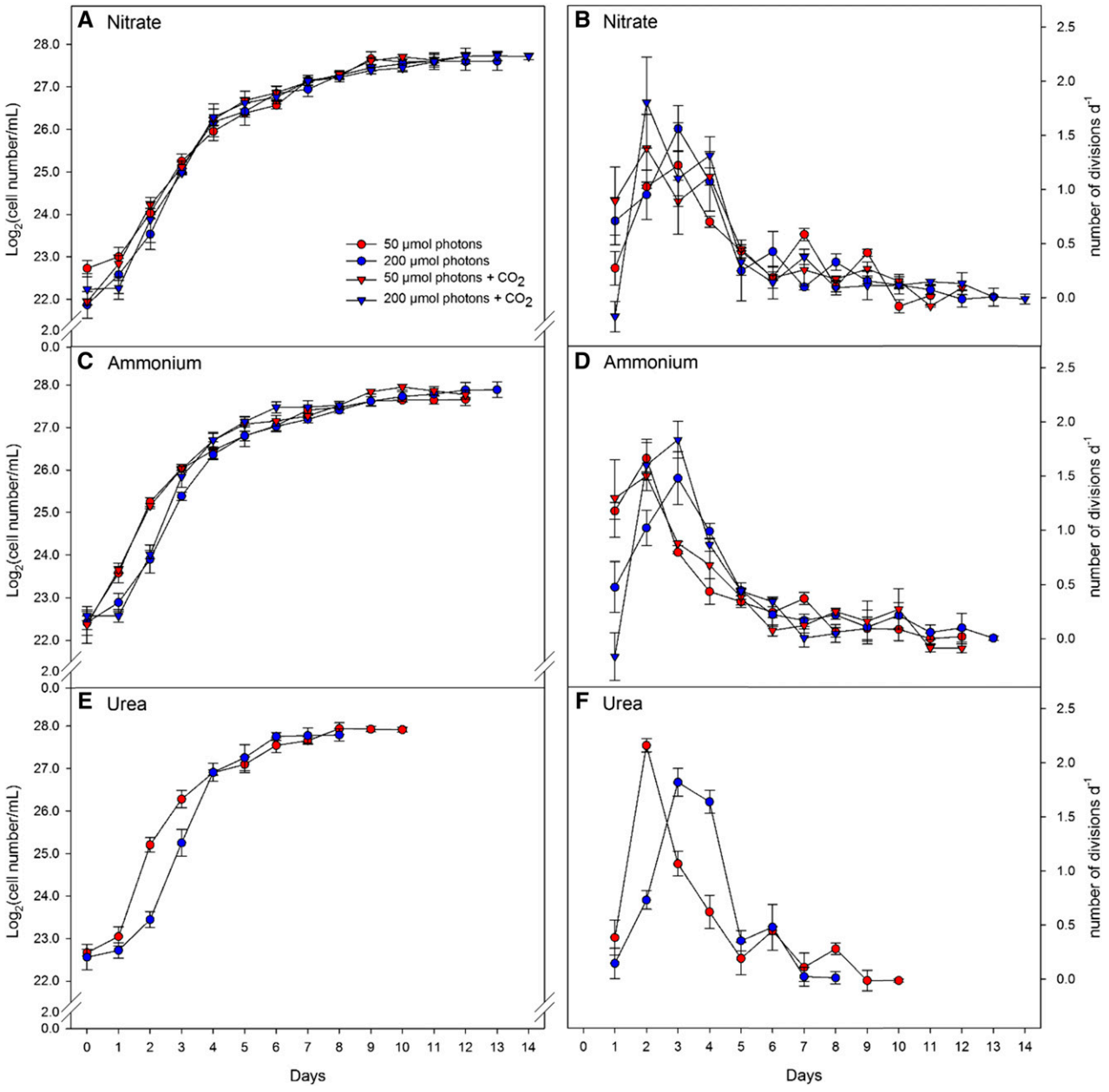

Figure 1. *Synechocystis* growth cycle represented on a log(cell) basis (A, C, and E) and daily number of divisions (B, D, and F) when grown on 10 different culture conditions. Cultures on nitrate (A and B), ammonium (C and D), and urea (E and F) were submitted to two different light intensities, 50 μmol photons m^{-2} s^{-1} (red) and 200 μmol photons m^{-2} s^{-1} (blue). Cultures grown on ammonium and nitrate were supplemented with 2.5 mM bicarbonate (triangles) or not supplemented (circles).

aim was to document the metabolic contents of the cells and relate this information to growth rates, the data were normalized on a per cell basis and not on a biomass basis. This method avoids biases due to specific growth conditions leading to cells containing more metabolites and then being heavier. Indeed, expressing our data on a biomass basis would have wrongly led to the conclusion of higher growth rates for some growth conditions, while, in fact, it could just be caused by cells accumulating more metabolites.

The rate of photosynthesis, as estimated by the determination of oxygen release, varied between the treatments (Table II). Under HL, cells grown in the presence of nitrate supplemented with CO_2, ammonium, and urea exhibited the highest photosynthetic rates (Table II). In addition, photosynthetic rates of cells cultured with ammonium and urea showed a light effect, with an increase by almost 60% when grown under HL (Table II). By contrast, nitrate cultures displayed similar photosynthetic rates and were not affected by

Downloaded from on August 30, 2017 - Published by www.plantphysiol.org
Copyright © 2017 American Society of Plant Biologists. All rights reserved.

Table I. *Gt of Synechocystis grown under 10 culture conditions*

Gt (hours) was calculated using a regression of the data within the logarithmic growth period at 50 μmol photons m^{-2} s^{-1} (ML) and 200 μmol photons m^{-2} s^{-1} (HL), with or without the addition of CO_2. Values represent means ± SD (n = 3). Means followed by the same letter do not differ by 5% probability (Tukey's test).

Culture	Gt	
	ML	HL
Nitrate	21.41 ± 1.26 fg	20.15 ± 1.63 efg
Ammonium	16.95 ± 0.57 abcd	19.30 ± 0.95 def
Urea	14.88 ± 0.61 abc	13.89 ± 0.20 a
Nitrate + CO_2	22.40 ± 0.17 g	17.91 ± 0.37 cde
Ammonium + CO_2	17.44 ± 2.26 bcde	14.70 ± 0.44 ab

increases in light intensity or CO_2 supplementation (Table II).

After 4 d of culture, the cellular dry weight (hereafter termed biomass) was higher under ML than HL for all the treatments, except for ammonium without CO_2 supplementation, for which the biomass did not differ (Supplemental Table S3). Chlorophyll *a* (hereafter termed chlorophyll) content was affected by nitrogen source and mostly by light intensity. In general, its content was higher under ML, in particular for cultures supplemented with nitrate (Supplemental Fig. S2A). The highest concentrations of phycocyanin were registered for cultures grown in the presence of nitrate and urea under ML, and the lowest concentrations were seen for cultures grown in the presence of ammonium and nitrate under HL (Supplemental Fig. S2B). Levels of total soluble sugars were almost constant among the different growth conditions (Supplemental Fig. S3A). As documented previously (Mikkat et al., 1997), Suc levels were below the level of detection, with the exception of cells grown on nitrate and the presence or absence of CO_2 under ML (Supplemental Tables S4 and S5). Total soluble sugars also were detected in the growth medium; however, their concentrations were similar for almost all treatments (Supplemental Fig. S4). Glycogen amounts at ED were relatively constant for all growth conditions, and only cells grown under HL and supplemented with CO_2 accumulated significantly more glycogen, independently of the nitrogen source (ammonium or nitrate; Supplemental Fig. S3B). A significant amount of the glycogen accumulated at ED was used during the night for all growth conditions (from 17.1% to 66.6%), except for cells grown in the presence of nitrate with ML (Supplemental Figs. S3B and S5). Levels of total soluble amino acids were very stable in cells grown under ML and did not exhibit diurnal variation. In contrast, their levels showed large variations between the treatments under HL (Supplemental Fig. S3C). The cellular protein content did not vary diurnally and was relatively similar between ammonium and urea growth conditions. Cells grown on nitrate displayed significantly higher protein content (Supplemental Fig. S3D). Cyanophycin levels did not vary diurnally and showed small variations between all growth conditions (Supplemental Fig. S3E).

In order to obtain insights into the carbon/nitrogen (C/N) balance and cellular redox status of the cells grown in the 10 contrasting growth conditions, we determined *ntcA* and *pII* expression (Supplemental Fig. S6). The relative expression levels of both genes showed no significant variations in response to the nitrogen source and CO_2 concentrations. On the other hand, their levels of expression at ED were negatively affected by the increase of the light intensity (Supplemental Fig. S6). In addition, *ntcA* and *pII* exhibit significant reductions in their expression at EN for all treatments (Supplemental Fig. S6).

Metabolic and Physiological Traits during the Stationary Phase

For most growth conditions, photosynthetic rates decreased by 50% to 60% at 3 d after the onset of the stationary phase (Table II), thus allowing the maintenance of a significant production of photoassimilates. Moreover, cells cultured in the presence of nitrate and ammonium (not supplemented with CO_2), under HL, kept similar rates of photosynthesis than those observed in log phase (Table II).

The biomass of cultures under ML exhibited a lower variation than under HL (Supplemental Table S3). The levels of chlorophyll and phycocyanin were similar in almost all of the growth conditions (Supplemental Fig. S7). Higher contents of total soluble sugars were observed for all cells grown under HL, especially for those grown in the presence of nitrate plus CO_2 and ammonium (Supplemental Fig. S8A). This makes sense, as these growth conditions were the ones in which photosynthetic rates remained high at stationary phase (Table II). By contrast, higher Suc levels were determined under ML (Supplemental Fig. S8B; Supplemental Tables S6 and S7). The highest levels of glycogen were observed in cultures grown in the presence of nitrate under ML. Glycogen degradation was significant for most of the growth conditions under HL (Supplemental Fig. S8C). As the photosynthetic rates were 2 times higher for some growth conditions without proportional increases of total soluble sugars and glycogen cellular contents (Supplemental Fig. S8, A and C), we next analyzed total soluble sugars in the culture medium. The highest levels of sugars in medium were measured for the three growth conditions where photosynthetic rates were maintained (Supplemental Fig. S9), suggesting that photosynthetic rates were higher than necessary for the growth demand and that the excess of photosynthate production is released to the medium. Total soluble amino acid content also was increased in cells grown under HL, independently of the nutrient treatments (Supplemental Fig. S10A). In good agreement with this, Glu levels were lower in these growth conditions (Supplemental Fig. S10B; Supplemental Tables S6 and S7). In addition, light intensity negatively affected cyanophycin accumulation (Supplemental Fig. S10C), while all treatments displayed similar protein contents (Supplemental Fig. S10D).

Downloaded from on August 30, 2017 - Published by www.plantphysiol.org
Copyright © 2017 American Society of Plant Biologists. All rights reserved.

Table II. *Photosynthetic rate in log and stationary phases*

Photosynthetic rate (μmol oxygen L^{-1} s^{-1} $cell^{-1}$) determined on the 4th day of culture (log phase) and 3 d after the onset of the stationary phase at 50 μmol photons m^{-2} s^{-1} (ML) and 200 μmol photons m^{-2} s^{-1} (HL), with or without the addition of CO_2. Statistics are as described for Table I.

Culture	Log		Stationary	
	ML	HL	ML	HL
Nitrate	$6.06 \times 10^{-10} \pm 2.50 \times 10^{-11}$ def	$5.44 \times 10^{-10} \pm 8.00 \times 10^{-11}$ cde	$2.28 \times 10^{-10} \pm 3.74 \times 10^{-11}$ a	$5.82 \times 10^{-10} \pm 6.33 \times 10^{-11}$ b
Ammonium	$4.61 \times 10^{-10} \pm 6.18 \times 10^{-11}$ abcd	$7.23 \times 10^{-10} \pm 4.69 \times 10^{-11}$ f	$2.75 \times 10^{-10} \pm 2.41 \times 10^{-11}$ a	$5.55 \times 10^{-10} \pm 5.23 \times 10^{-11}$ b
Urea	$3.89 \times 10^{-10} \pm 2.92 \times 10^{-11}$ ab	$6.20 \times 10^{-10} \pm 7.56 \times 10^{-11}$ ef	$2.23 \times 10^{-10} \pm 9.63 \times 10^{-12}$ a	$3.70 \times 10^{-10} \pm 1.11 \times 10^{-10}$ a
Nitrate + CO_2	$5.29 \times 10^{-10} \pm 2.92 \times 10^{-11}$ bcde	$5.72 \times 10^{-10} \pm 7.41 \times 10^{-11}$ def	$3.15 \times 10^{-10} \pm 7.82 \times 10^{-12}$ a	$6.09 \times 10^{-10} \pm 1.10 \times 10^{-11}$ b
Ammonium + CO_2	$4.01 \times 10^{-10} \pm 2.47 \times 10^{-11}$ abc	$3.18 \times 10^{-10} \pm 3.64 \times 10^{-11}$ a	$2.59 \times 10^{-10} \pm 1.36 \times 10^{-11}$ a	$3.02 \times 10^{-10} \pm 6.66 \times 10^{-11}$ a

The Decrease in Division Rates Seems to Be Unrelated to Nutrient Limitation, Quorum Sensing, or Self-Shading

To evaluate the possible influence of nutrient depletion and/or quorum sensing, we transferred cells from a whole culture that had reached stationary phase to fresh medium (Fig. 2). Cell density did not increase significantly (Table III; Supplemental Tables S8 and S9). In order to assess if the old medium obtained from the culture that had reached stationary phase was suboptimal for growth, we grew 3 mL of inoculum from the same resuspended pellet in the old medium (Fig. 2). After 4 d of culture, cell density increased 11 to 22 times, with the division rates being statistically similar to the rates observed when an inoculum of the same density was gown on fresh medium (Table III; Supplemental Tables S8 and S9). Besides, the whole growth cycle observed using the old medium appeared very similar to the one observed on fresh medium, and only when we attempted to reuse the medium for a third growth cycle we could observe a sharp decrease in division rates. High daily cell division rates were restored by the addition of fresh nutrients to the medium, but not by the addition of water (Fig. 3). Thus, the slow growth rates at stationary phase seem likely not due to a nutrient limitation, as our metabolic data suggested, nor to quorum sensing, as the growth of an inoculum would have been impaired in old medium due to the presence of a signal molecule, although we cannot exclude the possibility that this molecule had been highly unstable.

To confirm the absence of quorum sensing in our culture conditions and also test the possibility of an effect of light intensity and/or quality due to the high density of the cell culture, we next inoculated cells into a microtube fixed at the bottom of a flask containing a culture that had reached stationary phase (Fig. 2). Importantly, we allowed the exchange of medium between the culture and the cells within the microtube by sealing a filter of 0.45 μm at the entrance of the microtube. After 4 d of culture under ML, cell density in the microtubes reached 60% of what was achieved by an inoculum in the presence of fresh medium (Table IV), so the cells divided only one time less. Moreover, when cells were grown under HL, we did not observe any difference with a fresh culture (Table IV). This indicates that quorum sensing is not responsible for the decrease of growth rates and for the onset of stationary phase in *Synechocystis*. Moreover, self-shading had a very moderate effect under ML and probably no effect under HL (Fig. 1; Supplemental Table S1).

Given that nutrient limitation, quorum sensing, and self-shading may not explain the gradual decrease of growth and the onset of stationary phase, we considered whether a regulation triggered by cell-cell interaction could be involved in this process. For this purpose, experiments were performed with cultures grown on urea under HL to avoid the moderate self-shading effect observed under ML. In order to test this hypothesis, we started cultures using inocula at different cell densities. Cultures initiated with higher cell density showed

Downloaded from on August 30, 2017 - Published by www.plantphysiol.org
Copyright © 2017 American Society of Plant Biologists. All rights reserved.

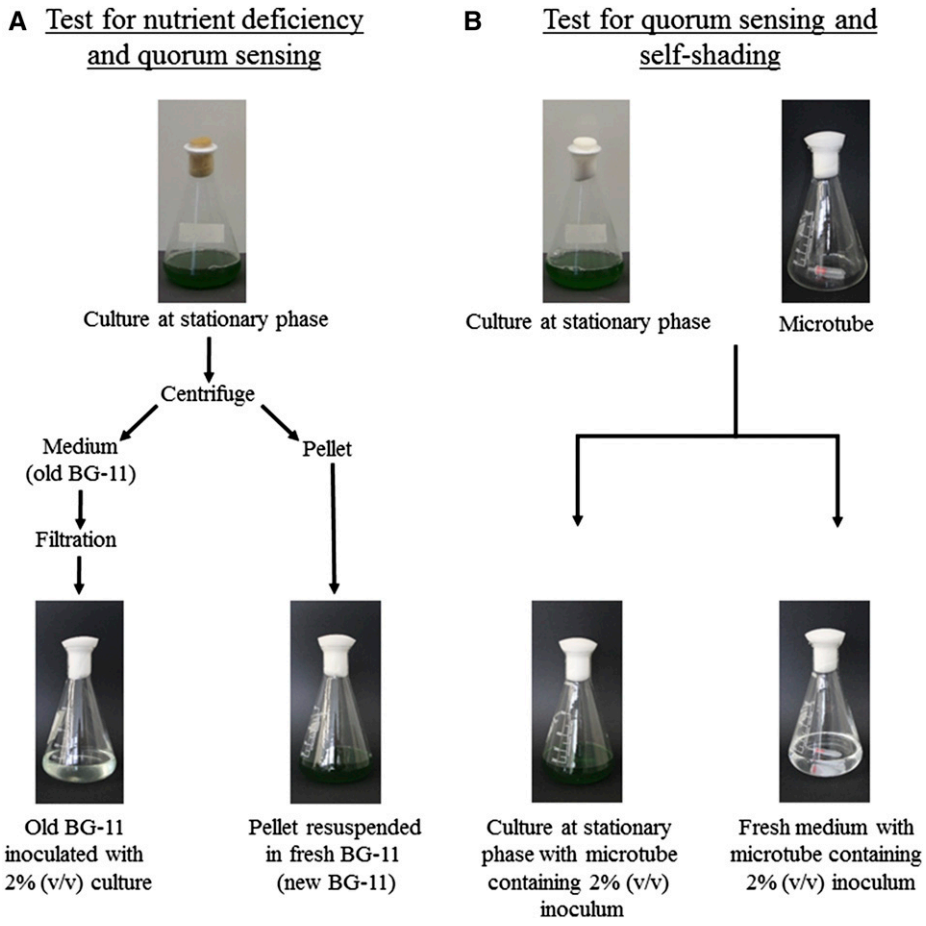

Figure 2. Experimental setup for the identification of the processes involved in the onset of stationary phase.

slower division rates during the 2nd and 3rd days of culturing, and all cultures exhibited a gradual decrease in their division rates from day 4 (Fig. 4, A and B).

In order to evaluate how fast the rate of cell division responded to an increase in cell density, we used centrifugation to artificially increase by a factor of 10 the density of log-phase cultures. This treatment led to 58% and 77% decreases in growth rates after 24 and 48 h, respectively. Cultures submitted to the same centrifugation process, but resuspended without being concentrated, did not present any alteration in their growth rate, dividing as fast as cultures that had not been centrifuged (Fig. 4, C and D).

In order to determine whether cell density quantitatively controls the rate of cell division, we grew *Synechocystis* in a fed-batch system at two different dilution rates. Cultures started with low cell density (4×10^6 cells mL^{-1}) and submitted to a dilution rate of 0.5× increased in

Table III. *Ratio between cell density at day 4 (D_4) and day 0 (D_0) of an inoculum grown on filtered medium from a previous culture that had reached stationary phase (condition 1) or whole-cell culture that had reached stationary phase and was regrown without dilution on fresh medium (condition 2)*

D_4:D_0 ratios were determined under 50 μmol photons m^{-2} s^{-1} (ML) and 200 μmol photons m^{-2} s^{-1} (HL), with or without the addition of CO_2. Control ratios were calculated from data obtained on growth curves shown in Figure 1 between the first 4 d of culturing (condition 1) and the last 4 d of culturing (condition 2). Values represent means ± SD ($n = 3$). The asterisk represents a significant difference between control and treatment for the same growth condition ($P < 0.05$, unpaired Student's t test). Cell densities for each growth condition and treatment are presented in Supplemental Tables S8 and S9.

Culture	Condition 1				Condition 2			
	Control		Filtered Medium Inoculated with 2% (v/v) Cells		Control		Cell Pellet Regrown on Fresh Medium	
	ML	HL	ML	HL	ML	HL	ML	HL
Nitrate	10.9 ± 1.1	19.7 ± 1.8	13.3 ± 3.6	14.4 ± 5.4	1.4 ± 0.1	1.1 ± 0.1	1.2 ± 0.2	1.2 ± 0.2
Ammonium	16.7 ± 0.4	15.5 ± 1.9	17.4 ± 3.4	11.9 ± 1.8	1.1 ± 0.1	1.3 ± 0.1	1.8 ± 0.4*	1.4 ± 0.3
Urea	18.9 ± 0.4	20.4 ± 1.3	22.9 ± 6.1	17. 8 ± 1.9	1.3 ± 0.1	1.8 ± 0.1	1.4 ± 0.3	1.6 ± 0.2
Nitrate + CO_2	19.5 ± 0.4	16.7 ± 2.3	14.6 ± 3.5	18.2 ± 0.4	1.3 ± 0.1	1.2 ± 0.1	1.3 ± 0.3	1.4 ± 0.2
Ammonium + CO_2	20.5 ± 4.2	17.5 ± 1.1	14.7 ± 2.0	19.0 ± 6.6	1.2 ± 0.1	1.8 ± 0.1	1.5 ± 0.2	1.7 ± 0.1

Downloaded from on August 30, 2017 - Published by www.plantphysiol.org
Copyright © 2017 American Society of Plant Biologists. All rights reserved.

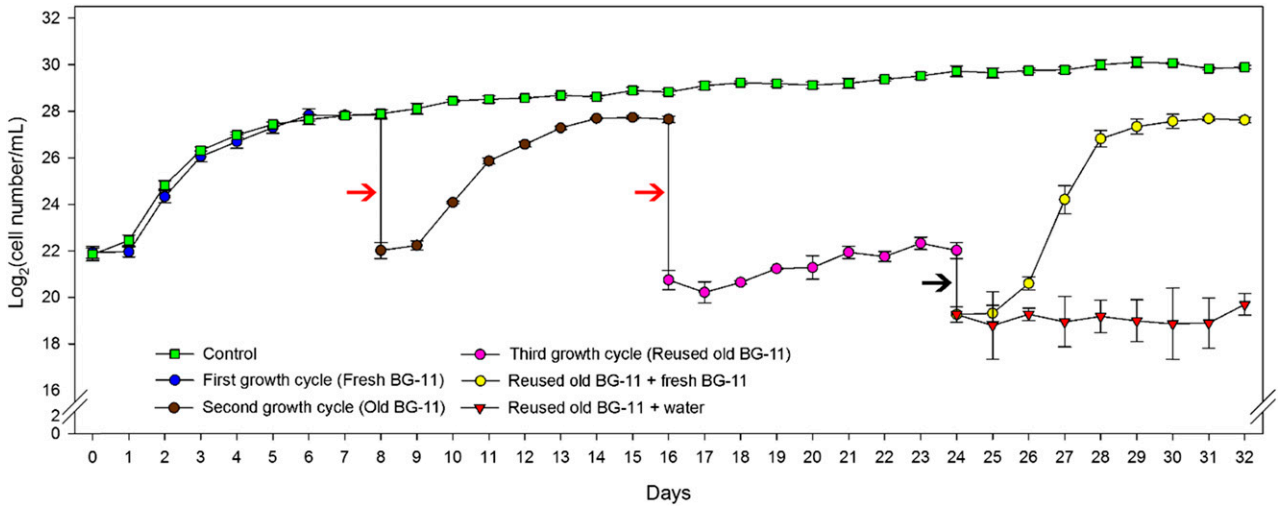

Figure 3. Growth cycles of *Synechocystis* on fresh BG-11 (blue circles), old BG-11 (brown circles), and reused old BG-11 (pink circles). Red arrows show when the entire culture was centrifuged and the supernatant was filtered and used to grow an inoculum, obtained from the resuspended pellet, during an additional 8 d. The black arrow shows when cultures with reused old BG-11 were divided in two parts and supplemented in a proportion of 1:1 with fresh BG-11 (yellow circles) or water (red triangles). As a control, cultures we maintained growing as a batch for the entire period of 32 d (green squares).

density during the first 4 d (Fig. 5, A and B). When cultures reached a density of 7×10^7 cells mL^{-1}, growth and dilution rate were counterbalanced and the culture density stayed stable, with cells dividing around 0.46 to 0.66 times per day for 7 d (Fig. 5, A and B). Next, we increased the dilution rate to two times per day. The cells divided faster than the dilution rate during the first 2 d, until the culture reached a density of 3.5×10^7 cells mL^{-1}, when cell division rate and dilution rate were counterbalanced. During the following days, the cells divided fast, with 1.7 to 2.2 divisions per day (Fig. 5, A and B).

Next, we investigated the effect of the same dilution rates on cultures that had reached stationary phase. At a dilution rate of 0.5× per day, cultures divided slower than the dilution rate on the first day, leading to a decrease of the cell density (Fig. 5, C and D). Then, cell division rates entered in balance with dilution, dividing 0.46 to 0.74 times per day during the following 6 d. When we applied a dilution rate of two times per day, we observed a gradual increase in cell division rates, which counterbalanced the dilution rate on the 3rd day of growth at a cell density around 2×10^7 cells mL^{-1}, with cells dividing 1.6 to 2.3 times per day for the next 6 d (Fig. 5, C and D). In summary, cell division rates appeared to be related directly to the cell density of the cultures.

DISCUSSION

Growth Rates Are Only Partially Controlled by the Metabolic Capacity and Mostly by the Cell Division Machinery

We built a Spearman's rank correlation matrix to identify potential metabolic and physiological traits that could be linked to growth and biomass (Fig. 6; Supplemental Fig. S11). Gt and biomass were significantly and positively correlated (r_s = 0.71; Fig. 6), meaning that cells dividing fast accumulate less biomass than cells dividing slowly. Photosynthesis did not correlate with growth and biomass. However, photosynthetic rates were positively correlated with amino acid levels at both ED and EN and with soluble sugar pools and glycogen at EN (Fig. 6). The absence of correlation between Gt and photosynthetic rate indicates that photosynthesis and growth were unrelated on the 4th day of culture, so 3 d after the start of the log phase for most of the culture conditions studied. This suggests that, instead of dividing, the cells store photoassimilates (Figs. 6 and 7). In agreement, Gt correlates positively with proteins and Suc at ED and EN and with glycogen, soluble sugars, citrate, and malate at EN. Additionally, we observed a strong negative correlation between cell number and protein and total soluble sugars at both ED and EN (Fig. 6). Thus, the gradual decrease in the division rate observed in our batch cultures (Fig. 1) does not appear to be due to a metabolic limitation but to a progressive decrease in the ability of cells to divide. Altogether, we observe uncoupling of Gt and photosynthetic rate, a progressive increase of both the carbon and nitrogen reserves, and, finally, the release of soluble sugars in the growth medium. The release of sugars to the medium can be seen as a strategy to avoid a possible inhibition of photosynthesis by negative sugar feedback (Oswald et al., 2001).

CO_2 supplementation did not promote increments in photosynthesis. Importantly, photosynthesis in this study is defined as oxygen release, which is related to the capacity to produce ATP and NADPH, and not to CO_2 assimilation. Therefore, we cannot exclude a higher Calvin-Benson cycle activity in the presence of higher

Downloaded from on August 30, 2017 - Published by www.plantphysiol.org
Copyright © 2017 American Society of Plant Biologists. All rights reserved.

Table IV. *Cell density of an inoculum grown in microtubes fixed at the bottom of flasks containing BG11 fresh medium (control) or a culture that had reached stationary phase (treatment)*

Cell number (cell number mL^{-1}) is shown for urea cultures grown under 50 μmol photons m^{-2} s^{-1} (ML) and 200 μmol photons m^{-2} s^{-1} (HL). Values represent means ± SD ($n = 3$). Asterisks represent significant differences between means for the same growth condition ($P < 0.05$, paired Student's *t* test).

Condition	ML			HL		
	Day 0	Day 4	Ratio (Day 4:Day 0)	Day 0	Day 4	Ratio (Day 4:Day 0)
Control	$5.69 \times 10^6 \pm 7.63 \times 10^5$	$4.31 \times 10^7 \pm 6.07 \times 10^6$*	7.58 ± 0.39	$3.40 \times 10^6 \pm 8.61 \times 10^5$	$3.81 \times 10^7 \pm 1.36 \times 10^7$*	11.00 ± 1.23
Treatment	$5.23 \times 10^6 \pm 8.19 \times 10^5$	$2.43 \times 10^7 \pm 2.86 \times 10^6$*	4.67 ± 0.33	$3.12 \times 10^6 \pm 2.89 \times 10^5$	$3.40 \times 10^7 \pm 7.90 \times 10^6$*	10.83 ± 1.62

CO_2 levels due to an inhibition of the photorespiratory pathway. However, it is highly unlikely, because we did not notice significant changes in cellular contents of Gly and Ser (Fig. 7; Supplemental Tables S4 and S5). An increase in light intensity only increased photosynthetic rates for cultures grown in the presence of ammonium and urea, and in fact, HL treatment mostly led to decreases in the amount of chlorophyll and phycocyanin (Table II; Supplemental Fig. S2). The lower pigment content observed under HL might lead to a lower redox state of the electron transport chain (Alfonso et al., 2000), which might be a strategy to avoid the production of reactive oxygen species and the inhibition of photosynthesis (Hihara et al., 2001; Muramatsu et al., 2009), particularly when photoassimilates cannot be used for cell division. Interestingly, Kopecná et al. (2012) showed that, even with a lower cellular chlorophyll content under HL, the rate of chlorophyll synthesis was higher than at lower light intensity. This was explained by a reduction of the half-life of chlorophyll molecules and a greater demand for chlorophylls as a result of faster growth rates.

pII and *ntcA* are major proteins involved in sensing C/N balance in cyanobacteria (Flores and Herrero, 2005). The expression levels of *ntcA* were not affected by nitrogen sources, as described previously (Alfonso et al., 2001). *pII* and *ntcA* transcript levels were positively correlated (r_s = 0.83; Supplemental Fig. S11), which was expected because *ntcA* controls *pII* expression (García-Domínguez and Florencio, 1997; Lee et al., 1999). *ntcA* and *pII* transcript levels correlated negatively with total amino acid levels and positively with chlorophyll, citrate, isocitrate, fumarate, malate, and Glu, in agreement with their role in sensing C/N balance (Supplemental Fig. S11). *pII* expression correlated positively with biomass (r_s = 0.83; Fig. 6) but not with Gt. This is likely explained by the positive correlation between Gt and biomass, showing that cells dividing slowly accumulate more biomass and, in particular, carbon-rich compounds. Thus, cells dividing slowly were not metabolically limited, although another factor clearly limits their growth.

When *Synechocystis* was grown in the presence of urea, it displayed fast division rates, one of the shortest growth cycles, and lower metabolite contents (Figs. 1 and 7; Table I), suggesting that urea may be a promising alternative to nitrate and ammonium for growing cyanobacteria species of biotechnological interest. In this condition, cells displayed higher photosynthetic rates when cultured under HL, although this did not lead to increased growth rates (Tables I and II). These data reinforce our observations that growth and photosynthesis are not directly linked. Moreover, even with a fast growth rate and lower reserves, cells may still present sink limitations to support the rate of photoassimilate synthesis, since the cellular levels of soluble sugars and their concentrations in the medium were similar to those observed under the other nine treatments (Supplemental Figs. S3A and S4).

Altogether, our metabolic and physiological data indicate the absence of a metabolic limitation of growth at

Downloaded from on August 30, 2017 - Published by www.plantphysiol.org
Copyright © 2017 American Society of Plant Biologists. All rights reserved.

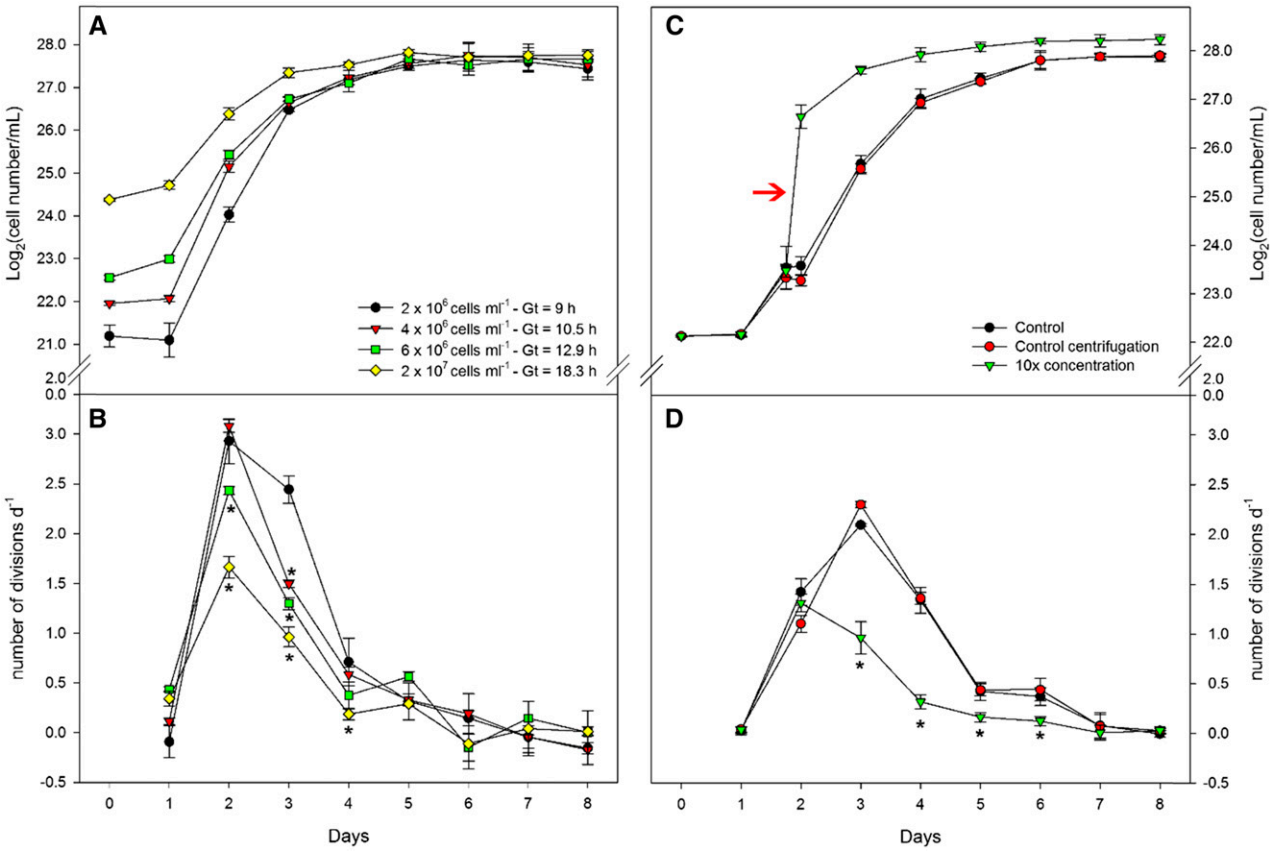

Figure 4. Experimental setups to test the effects of cell density on *Synechocystis* growth. A and B, Effects of different initial cell densities on growth cycle (A) and daily number of divisions (B): 2×10^6 (black), 4×10^6 (red), 6×10^6 (green), and 2×10^7 (yellow) cells mL^{-1}. C and D, Effects of an artificial increase of cell density on growth cycle (C) and daily number of divisions (D). The red arrow in C indicates an artificial increase of cell density. Control cultures (black) were not disturbed during their growth; control centrifugation cultures (red) were submitted to the same pipetting, centrifugation, and growth conditions of 10× concentration but not concentrated after centrifugation; 10× concentration cultures (green) were artificially concentrated after centrifugation. Asterisks represent significant differences from 2×10^6 cells mL^{-1} (B) or control (D) at $P < 0.05$ (Student's *t* test).

log phase. The photosynthetic rates observed were high enough to support the synthesis of sugars and amino acids required for growth, which, instead of being used for it, were redirected for the synthesis of storage proteins. Indeed, at day 4 of culture, the protein content was positively correlated with Gt and negatively with the number of cells, suggesting that a major fraction of proteins was used as nitrogen storage. Moreover, a significant amount of sugars was released to the growth medium instead of being used by the cellular metabolism.

Is Stationary Phase Reached Because of Metabolic/ Nutrient Limitation?

Cultures grown under the different growth conditions reached stationary phase with similar cell densities (Supplemental Table S1), despite varying durations of culture due to slightly different division rates (Fig. 1; Table I). This suggests that a nonmetabolic factor is responsible for the onset of stationary phase. In order to provide further support for the above hypothesis, we investigated the role of metabolism, nutrients, quorum sensing, and self-shading in the onset of stationary phase.

At stationary phase, the rate of photosynthesis remained high compared with that observed at log phase, decreasing by 50% to 60% under ML and being largely unaffected under HL (Table II). The decrease under ML is likely explained by self-shading, and this difference between HL and ML led to dramatic differences in the metabolic profiles of cells grown under ML and HL. The rate of photosynthesis correlated negatively with Glu at both ED and EN and positively with total soluble sugars (in cells and culture medium), proteins, total soluble amino acids, as well as the levels of some individual amino acids, such as Leu, Ile, Ala, Gly, and Phe at ED and Pro at both ED and EN (Fig. 8). Total soluble amino acids correlated negatively with chlorophyll, cyanophycin, citrate, isocitrate, and Glu and positively with total soluble sugars (in cells and culture medium), proteins, and Pro (Fig. 8). The

Downloaded from on August 30, 2017 - Published by www.plantphysiol.org
Copyright © 2017 American Society of Plant Biologists. All rights reserved.

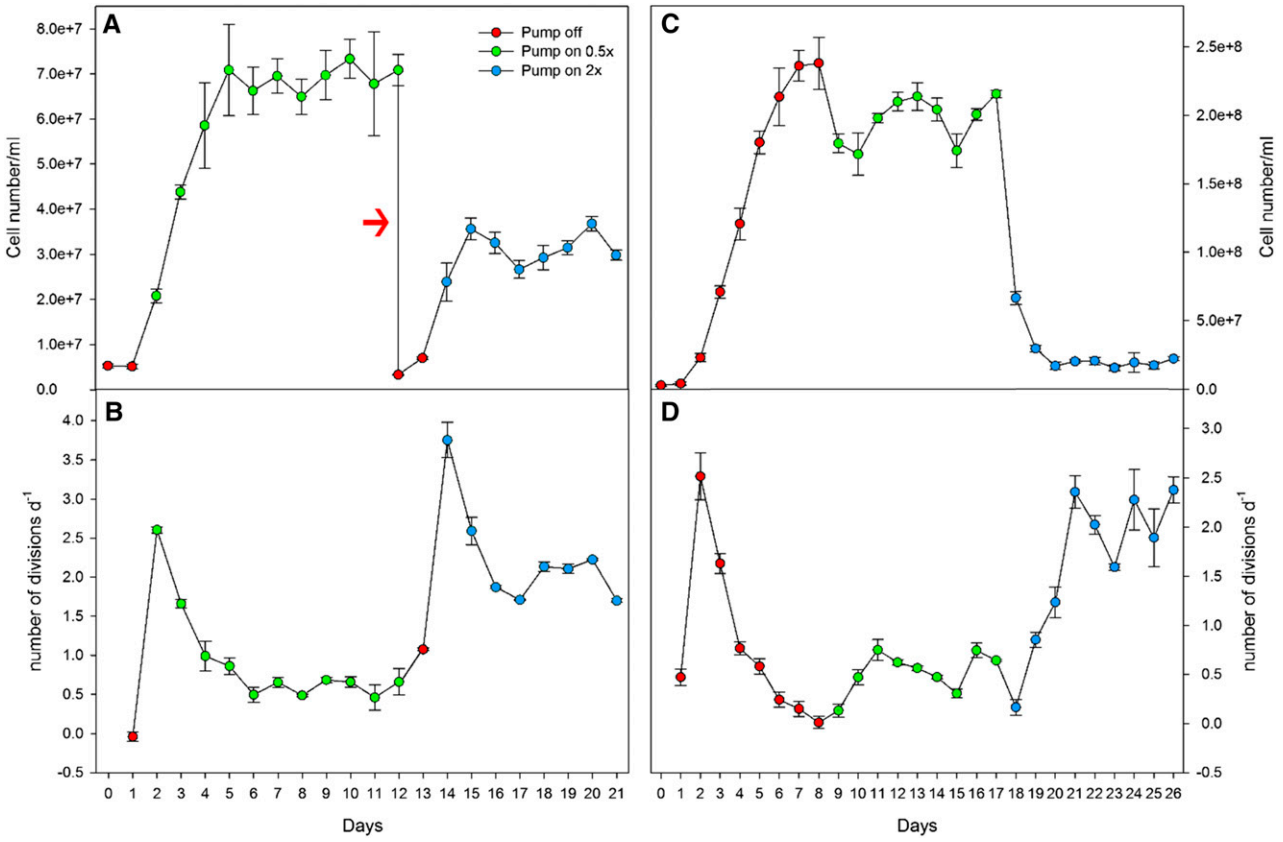

Figure 5. Experimental setups to test the effects of cell density on *Synechocystis* growth. Growth cycle and daily number of divisions are shown for cultures grown in fed-batch condition starting at low cell density (A and B) and high cell density (C and D). The red arrow in A indicates that cultures were diluted to the same initial density of day 0.

negative correlations of amino acids with citrate, isocitrate, and Glu suggested that these metabolites had been used mainly as a source of carbon skeleton for amino acid synthesis. Additionally, the correlations of total amino acids and soluble sugars with proteins (r_s = 0.7 and 0.79, respectively) and cyanophycin (r_s = −0.82 and −0.62, respectively) indicate that protein synthesis was the main sink of these metabolites (Fig. 8; Supplemental Fig. S12). Moreover, positive correlations between Arg, proteins, and biomass, at this stage, were observed (Fig. 8; Supplemental Fig. S12).

As the photoassimilates were not used for growth, we observed an accumulation of soluble sugars, concomitant to an accumulation of amino acids, and enhanced export of sugars to the culture medium (Fig. 8). Because of the higher export of sugars to the medium under HL than ML, the levels of Suc in cells under HL were much lower than under ML (Supplemental Fig. S8B). This disaccharide is described as a compatible solute with no net charge, and it is proposed that it can be accumulated without interfering in cellular homeostasis (Brown, 1976; Mackay et al., 1984; Mikkat et al., 1997; Miao et al., 2003; Hagemann, 2011). However, our data suggest that Suc might have an effect on cellular homeostasis, and in particular photosynthesis, possibly by sugar feedback inhibition of photosynthesis (Stitt et al., 1991). Indeed, in contrast to ML, cells grown under HL could maintain a high level of photosynthesis while exporting larger amounts of Suc in the medium and accumulating much lower amounts of Suc within their cells. Altogether, the correlations suggest that stationary phase was not achieved due to a limitation in the availability of building blocks and/or energy necessary to maintain cell division.

Considering that the metabolism does not control the rate of cell division, we tested whether already known factors were responsible, such as (1) nutrient starvation (Lazazzera, 2000; Berla and Pakrasi, 2012), (2) quorum sensing (Sharif et al., 2008), and (3) reduction of light quality and intensity available to the cells due to high cell density (self-shading; Raven and Kübler, 2002; Ort and Melis, 2011; Lea-Smith et al., 2014).

Nutrient deficiency could not account for the gradual decrease of cell division rate because (1) a whole culture that had reached stationary phase did not restart its growth when transferred to a fresh medium and (2) when we grew an inoculum into the medium obtained from a culture at stationary phase, the inoculum could grow at the same rate as in fresh medium, and an inhibition of growth was observed only if we attempted

Downloaded from on August 30, 2017 - Published by www.plantphysiol.org
Copyright © 2017 American Society of Plant Biologists. All rights reserved.

	Day				Night			
	Gt	Biomass	*A*	Cell number	Gt	Biomass	*A*	Cell number
Gt								
Biomass	0.71				0.71			
A	0.33	0.04			0.33	0.04		
Cell number	-0.93	-0.56	-0.35		-0.93	-0.56	-0.35	
Chlorophyll *a*	0.56	0.72	0.04	-0.43	0.54	0.75	-0.03	-0.35
Phycocyanin	0.36	0.53	0.27	-0.33	0.12	0.05	0.37	-0.18
Proteins	0.85	0.56	0.52	-0.90	0.94	0.59	0.41	-0.88
Total amino acids	0.33	-0.09	0.72	-0.42	0.36	0.12	0.75	-0.41
Cyanophycin	0.16	-0.21	0.25	-0.31	0.50	0.24	0.55	-0.55
Glycogen	-0.27	-0.37	-0.26	0.13	0.70	0.21	0.73	-0.71
% degraded glycogen					-0.90	-0.84	-0.14	0.84
Total soluble sugars (cell)	0.56	0.26	0.38	-0.72	0.66	0.21	0.73	-0.71
Sucrose	0.68	0.63	0.08	-0.52	0.68	0.63	0.08	-0.52
Total soluble sugars (media)					0.27	-0.01	0.26	-0.42
Maltose	0.18	0.52	-0.45	-0.20	-0.39	0.03	-0.43	0.28
Citrate	0.38	0.59	-0.16	-0.48	0.64	0.44	0.27	-0.75
Isocitrate	0.25	0.46	-0.43	-0.10	-0.21	0.08	-0.38	0.24
Glutamate	0.56	0.72	-0.03	-0.56	0.20	0.47	0.15	-0.13
Ornithine	0.38	0.44	-0.27	-0.48	-0.25	-0.18	-0.09	0.01
Aspartate	0.50	0.38	-0.19	-0.57	-0.38	-0.68	0.37	0.19
Arginine	-0.01	0.22	-0.31	-0.18	-0.20	-0.44	-0.07	-0.10
Fumarate	0.48	0.80	-0.14	-0.42	0.59	0.60	0.20	-0.65
Malate	0.48	0.80	-0.14	-0.42	0.67	0.56	0.42	-0.73
Proline	0.41	0.49	-0.24	-0.50	0.35	0.04	0.56	-0.55
Leucine	0.36	0.31	-0.09	-0.50	0.14	-0.16	0.43	-0.35
Isoleucine	0.38	0.24	0.08	-0.52	-0.07	-0.42	0.39	-0.14
Valine	0.43	0.50	-0.22	-0.53	0.05	-0.27	0.35	-0.26
Alanine	0.09	0.14	-0.43	-0.23	0.07	-0.12	0.27	-0.31
Glycine	0.38	0.50	-0.27	-0.45	-0.16	-0.32	0.35	0.01
Serine	0.42	0.60	-0.22	-0.47	-0.01	-0.30	0.31	-0.20
Tyrosine	0.31	0.39	-0.28	-0.44	-0.27	-0.65	0.30	0.05
Lysine	0.24	0.60	-0.41	-0.26	-0.36	-0.20	-0.03	0.16
Tryptophan	0.20	0.09	-0.09	-0.45	-0.07	-0.45	0.62	-0.08
Phenylalanine	0.45	0.45	-0.14	-0.55	-0.07	-0.31	0.43	-0.18
Glycolate	0.54	0.89	-0.30	-0.43	0.22	0.32	-0.38	-0.13
Glycerate	0.41	0.84	-0.30	-0.26	0.10	0.47	-0.36	-0.07
Nicotinate	0.58	0.82	-0.31	-0.48	0.45	0.67	0.07	-0.31
Nicotinamide	0.44	0.76	-0.36	-0.38	0.13	0.58	-0.04	-0.08
Alpha-tocopherol	0.45	0.63	0.15	-0.37	0.71	0.71	0.28	-0.56
ntcA	0.16	0.58	-0.45	-0.14	-0.42	-0.22	0.20	0.49
pII	0.31	0.81	-0.44	-0.22	-0.10	0.19	0.24	-0.03

Figure 6. Spearman's rank coefficient of correlation between Gt, biomass, photosynthetic rate (*A*), and cell number, and metabolite and gene expression levels determined at ED and EN on the 4th day of culture. Total soluble sugars (medium) was determined only at EN. Significant correlations at 5% probability are highlighted in green (positive) and red (negative). Additional correlations between all growth, physiologic, metabolic, and molecular traits are presented in Supplemental Figure S11.

to reuse the medium a third time (Fig. 3; Table III; Supplemental Tables S8 and S9). For the same reason, low cell viability could not account for the decrease in cell division. Our conclusion differs from that of Schuurmans et al. (2017), who concluded that the transition to stationary phase is caused by nutrient limitation. However, the authors artificially stopped growth by bubbling cultures with nitrogen gas (N_2), which deprived cells of CO_2 and oxygen and, indeed, led to carbon starvation and growth arrest. However, this does not mean that a culture not deprived of CO_2 and oxygen would reach stationary phase for the same reason.

Quorum sensing is unlikely responsible because (1) an inoculum could grow normally on a medium obtained from a culture that had reached stationary phase (Table III) and (2) an inoculum in a microtube fixed at the bottom of a culture that had reached stationary phase could grow almost normally under ML and normally under HL (Table IV). This second observation also led us to conclude that light intensity and quality had minor impacts on the onset of stationary phase. Moreover, cell density reached at stationary phase was the same for nine out of the 10 growth conditions we tested and, thus, independent of the two contrasting light intensities we applied (Fig. 1; Supplemental Table S1). Schuurmans et al. (2017) showed that a gradual increase of light intensity can lead cells to divide faster and avoid a linear phase. Based on this observation, the authors affirmed that the decrease of cell division from log to linear phase is caused solely by light limitation (self-shading). The authors used 30 μmol photons m^{-2} s^{-1} and, indeed, cells might have been light limited, thus leading to lower CO_2 assimilation and limitation of the photoassimilates available for growth. Moreover, the authors stopped their experiment after 72 h by bubbling N_2, which led to acute carbon starvation and growth arrest, while in our study, we observed delayed growth due to cell density after 72 to 96 h of growth. Based on our results, we suggest that cells can continue growing after 72 h and then will exhibit a gradual decrease of their growth rates, reaching linear phase before the onset of stationary phase, irrespective of the light intensity.

Our results indicate that cell density may negatively affect the growth rates of cultures at relatively high densities, as an artificial increase of density by 10 times led to a decrease in the daily growth rate by 58% after 24 h ($P < 0.001$) and 77% after 48 h ($P < 0.0001$; Fig. 4, C and D). Moreover, cell density seems to be involved in the control of growth rates, as demonstrated by fed-batch data. Indeed, we could stabilize cell division over several days by maintaining cells at two given densities, applying different dilution rates. Interestingly, a dilution rate of 0.5× per day led to a division rate of 0.5 times per day, while a dilution rate of 2× per day led to two divisions per day (Fig. 5, C and D), which is close to the maximal division rates we observed in our batch cultures and in line with Kim et al. (2011). Moreover, when applying a dilution rate of 2×, we first observed higher division rates (around four divisions per day), which is close to those reported by Hihara et al. (2001) and Zavřel et al. (2015). This fast growth rate led to an increase in the density of the culture before the division rates stabilize and quantitatively counterbalanced the daily dilution applied. Altogether, these data suggest that cell density is involved in the control of the division rates in *Synechocystis*.

It is important to highlight that the observations in fed-batch cultures are not an effect of fresh nutrients on

Downloaded from on August 30, 2017 - Published by www.plantphysiol.org
Copyright © 2017 American Society of Plant Biologists. All rights reserved.

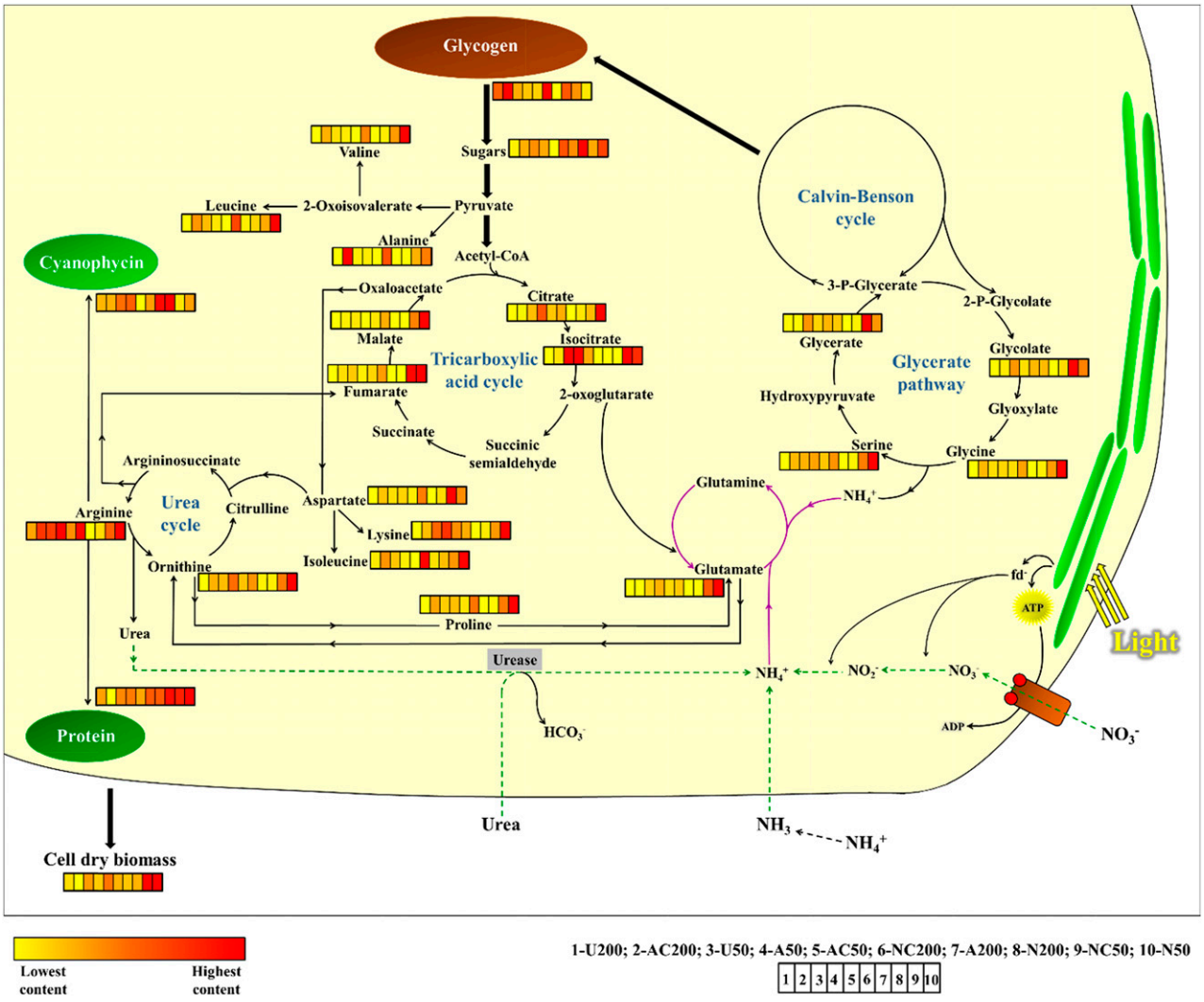

Figure 7. Heat map of metabolite levels. Culture conditions are ordered based on growth rates, from the fastest (left) to the slowest (right). A, Ammonium; C, CO_2; N, nitrate; U, urea; 50, 50 μmol photons m^{-2} s^{-1}; 200, 200 μmol photons m^{-2} s^{-1}.

growth, since previous data indicate that medium from cultures at stationary phase contain enough nutrients to support a second entire growth cycle with similar growth rates (Fig. 3). Even though self-shading showed a moderate effect at ML (Table IV), we propose that a cell-cell interaction process (Belas, 2014; Ellison and Brun, 2015) is involved in the control of cell division rate and that this mechanism may be responsible for the gradual decrease in daily growth rates until the onset of stationary phase, when cells are cultured in batch. At stationary phase, cells can still divide at very slow rates and reach higher densities. Cultures maintained for 24 d after the onset of stationary phase reached cell densities around 1.2×10^9 cells mL^{-1} (Fig. 3). However, during this period, cells only divided 3.5 times.

Even though our data suggest that a mechanism involving cell-cell interaction is possibly involved in the control of division rates of *Synechocystis* when grown planktonically, this regulation seems absent when cells are grown on agar. Indeed, *Synechocystis* normally forms dense colonies on agar, exhibiting log growth and fast doubling times of approximately 8 h (Law et al., 2000; Lamb et al., 2014). This observation suggests that *Synechocystis* growth regulation differs when cultured on an agar surface or in liquid. Data from the literature show that heterotrophic bacteria exhibit different gene expression patterns in biofilm and in planktonic growth (Imanaka et al., 2010; He and Ahn, 2011; Romero-Lastra et al., 2017). Among the genes that are up-regulated under biofilm conditions, some encode proteins located in the outer membrane or cell envelope and involved in transport or binding (Romero-Lastra et al., 2017). Furthermore, a significant number of the genes differentially expressed encode for proteins of unknown functions (Imanaka et al., 2010). Compared with heterotrophic bacteria, there is little information about biofilm formation in cyanobacteria (Parnasa et al., 2016). However, recent studies have

Downloaded from on August 30, 2017 - Published by www.plantphysiol.org
Copyright © 2017 American Society of Plant Biologists. All rights reserved.

	Day			Night		
	Biomass	*A*	Total amino acids	Biomass	*A*	Total amino acids
Biomass						
A	0.36			0.36		
Total amino acids	-0.02	**0.68**		0.30	**0.88**	
Cell number				-0.28	-0.21	-0.41
Chlorophyll	0.37	-0.55	**-0.83**	0.61	-0.22	-0.24
Phycocyanin	**0.82**	0.02	-0.21	**0.90**	0.20	0.12
Proteins	0.59	**0.71**	**0.70**	**0.96**	0.47	0.39
Cyanophycin	0.36	-0.50	**-0.82**	0.41	-0.49	**-0.67**
Glycogen	0.50	-0.10	0.10	0.55	-0.30	-0.35
Total soluble sugars (cell)	0.14	**0.88**	**0.85**	0.48	**0.88**	**0.87**
Sucrose	0.49	-0.35	-0.61	0.44	-0.36	-0.45
Total soluble sugars (media)				0.15	**0.78**	**0.71**
Maltose	0.45	-0.27	-0.62	0.55	-0.17	-0.09
Citrate	0.04	-0.37	**-0.82**	0.21	-0.50	-0.56
Isocitrate	-0.12	-0.38	**-0.67**	0.09	-0.54	-0.52
Glutamate	-0.04	**-0.68**	**-0.81**	-0.19	**-0.78**	**-0.77**
Ornithine	0.33	0.62	0.19	0.58	0.30	0.26
Aspartate	-0.05	0.44	0.28	0.15	0.31	0.49
Arginine	0.35	0.28	0.02	**0.67**	0.32	0.37
Fumarate	0.26	0.22	-0.28	0.41	-0.04	-0.12
Malate	0.14	-0.02	-0.14	0.41	-0.01	-0.08
Proline	0.32	**0.78**	**0.75**	0.31	**0.88**	**0.98**
Leucine	-0.01	**0.72**	0.59	0.27	0.45	0.58
Isoleucine	0.14	**0.78**	0.58	0.31	0.44	0.54
Valine	0.16	0.53	0.31	0.28	0.39	0.55
Alanine	0.04	**0.85**	**0.73**	0.43	0.48	0.62
Glycine	0.14	**0.68**	0.49	0.28	0.45	0.59
Serine	-0.05	0.42	0.20	0.15	0.07	0.16
Tyrosine	0.03	0.47	0.13	0.36	0.30	0.24
Lysine	-0.10	0.45	0.20	0.19	0.36	0.41
Tryptophan	0.05	0.33	0.05	0.21	-0.24	-0.28
Phenylalanine	0.16	**0.76**	0.54	0.42	0.44	0.59
Glycolate	0.28	0.43	0.60	0.30	0.37	0.56
Glycerate	-0.07	-0.09	0.05	-0.22	-0.49	-0.42
Nicotinate	0.54	0.59	**0.66**	0.32	**0.72**	**0.92**
Nicotinamide	0.48	-0.13	-0.42	0.49	-0.03	0.08
Alpha-tocopherol	**0.75**	0.27	-0.08	**0.84**	0.58	0.60

Figure 8. Spearman's rank coefficient of correlation between biomass, photosynthetic rate (*A*), and total amino acids, and metabolite levels determined at ED and EN in cells 3 d after the onset of the stationary phase. Total soluble sugars (medium) was determined only at EN. Significant correlations at 5% probability are highlighted in green (positive) and red (negative). Additional correlations between all growth, physiologic, metabolic, and molecular traits are presented in Supplemental Figure S12.

shown that *Synechocystis* and *Synechococcus elongatus* PCC 7942 also exhibit variations in gene expression pattern when grown on a solid surface or in liquid (Nakasugi and Neilan, 2005; Schatz et al., 2013; Agostoni et al., 2016). Interestingly, the *Synechocystis* strain used in this study, which is not identified as Glc tolerant, grew well in liquid BG11 supplemented with Glc concentrations from 0.2 to 20 mM (Supplemental Fig. S13). However, as observed by Williams (1988), colonies of the strain could not grow on agar containing more than 0.2 mM Glc (Supplemental Fig. S13). It is thus possible that *Synechocystis* exhibits variations in its regulation of growth when grown on solid or liquid medium and that the control of growth via cell-cell interaction we observed in liquid medium does not occur on solid medium.

This process of cell-cell interaction might be a strategy to avoid competition for nutrients and light and, thus, starvation and death. If cells keep a constant rate of cell division, they would become limited by light and nutrients due to depletion of the nutrients in the environment and self-shading. Thus, they would die due to starvation, since their cellular reserves are finite. Hence, a natural selection of individuals able to sense a gradual increase in density and regulate their division rates accordingly. Besides, cells that did not have this mechanism and exhibited an unrestricted growth probably would be more susceptible to environmental variations, as they would likely have less reserves to buffer environmental variations. Our conclusions, therefore, vary significantly from what is usually observed in nonphotosynthetic bacteria, where starvation and quorum sensing are responsible for the onset of stationary phase (Lazazzera, 2000; Shiloach and Fass, 2005).

CONCLUSION

Our data suggest that cell-cell interaction possibly affects growth and promotes a gradual decrease of the division rate during the log phase. As a consequence, the photoassimilates start to be stored instead of being used for growth, leading to a decoupling between growth and photosynthesis. This storage of metabolites decreases the cellular sink capacity, and cells start to export sugars to the medium as an alternative to avoid an inhibition of photosynthesis by negative feedback. As the growth rates in batch cultures seem to be regulated primarily by cell density, dilutions are necessary to maintain fast division rates for a long period. Our conclusions not only have biotechnological implications but also suggest that studies investigating major drivers of the metabolic control of growth should be performed with care at culture densities where a possible growth inhibition by cell density does not occur, ideally in fed-batch or continuous cultures in order to precisely control cell densities and then cell division rates. Another outcome of this study is that urea is a valuable nitrogen source, as we could get high division rates and short growth cycles. This nitrogen source can be an alternative to grow some cyanobacteria as an economically viable biomass production, since urea is cheaper than ammonium and nitrate, its transport does not require metabolic energy, and during its assimilation there is a release of CO_2 into the cell.

Downloaded from on August 30, 2017 - Published by www.plantphysiol.org
Copyright © 2017 American Society of Plant Biologists. All rights reserved.

MATERIALS AND METHODS

We selected the strain *Synechocystis* sp. PCC 6803 for our study since it is a major cyanobacterial model with a very large amount of literature available about its physiology and molecular characteristics. The strain was obtained directly from the French Pasteur Culture Collection (PCC strain) and shows positive phototaxis when grown on BG-11 agar plates (Kanesaki et al., 2012).

Growth Conditions

Synechocystis was cultivated under two light intensities (50 and 200 μmol photons m^{-2} s^{-1}), two CO_2 concentrations (ambient and 2.5 mM bicarbonate), and three nitrogen sources (nitrate, ammonium, and urea), for a total of 10 different growth conditions. All cultures were grown under an 18-h/6-h day/night photoperiod, at a constant temperature of 26°C ± 1°C, and constantly shaken at 120 rpm. To allow complete acclimation to each treatment, *Synechocystis* was cultivated three times from log to stationary phase in all growth conditions before analyses were performed.

Cultures were initiated with 3 mL of inoculum in a conical flask (500 mL) containing 147 mL of BG-11 medium (2%, v/v; Rippka et al., 1979), for a starting cell density ranging from 4 to 6×10^6 cells mL^{-1}. $BG\text{-}11_0$ (without nitrogen) was supplemented with sodium nitrate (17.7 mM) or ammonium (5 mM) or urea (2.5 mM). Due to the release of CO_2 when urea is hydrolyzed, the same concentration of CO_2 (2.5 mM) was added in ammonium and nitrate cultures in the form of sodium bicarbonate ($NaHCO_3$; hereafter CO_2). To maintain the pH at 7.5 ± 0.5, HEPES (20 mM) was added in the medium.

Estimation of Gt

Growth cycle was evaluated by counting cells in a Neubauer chamber (Optik Labor) at intervals of 24 h, until the third subsequent day showing no significant increases in cell density (stationary phase). The Gt for each treatment was calculated using a regression of the data within the logarithmic growth period.

Experimental Protocols to Test Nutrient Limitation, Quorum Sensing, and Self-Shading

To evaluate the possibility that nutrient depletion and/or quorum sensing affect cell density at stationary phase, *Synechocystis* was cultured for 15 d in the different growth conditions described above in order to reach stationary phase. Then, all the volume was centrifuged. The pellet was resuspended in a fresh BG-11 medium (new BG-11), and the volume was adjusted to 150 mL. The supernatant (old BG-11) was filtered on a nitrocellulose membrane (47 mm × 0.22 μm; Sarstedt) and inoculated with 3 mL of the respective resuspended pellet. Cell density was determined and cultures were grown in the same conditions as previously. After 4 d of cultivation, the cellular density was determined to assess growth rates.

One growth condition, urea as the nitrogen source and a light intensity of 200 μmol photons m^{-2} s^{-1}, for which maximum growth rates were achieved, was selected to evaluate how many growth cycles of *Synechocystis* BG-11 could support. *Synechocystis* was cultured for 8 d in fresh BG-11 until the onset of stationary phase. Subsequently, the entire culture was centrifuged and the supernatant (old BG-11) was filtered and used to grow an inoculum obtained from the resuspended pellet for an additional 8 d. At the end of this period, cultures were centrifuged and the supernatant was filtered and reused again (reused old BG-11) to culture for 8 d an inoculum obtained from the previous pellet. Finally, cultures were divided into two equal volumes, supplemented in a proportion of 1:1 with fresh BG-11 or water, and kept growing for an additional 8 d.

To test for quorum sensing and light quality/intensity, cultures of *Synechocystis* were cultivated on urea at 50 or 200 μmol photons m^{-2} s^{-1} for 15 d in order to obtain cultures at saturation phase. For both light intensities, three translucent microtubes (2 mL) were filled with 1.5 mL of BG-11 culture medium (supplemented with urea) containing 2% (v/v) of the respective *Synechocystis* culture. These tubes were glued at the bottom of conical flasks (500 mL) after being sealed with filters (Sigma Iso-Disc Filters PFTE-4-4; 4 mm × 0.45 μm). The filters allowed for medium exchange, but cells could not go in or out. Then, the conical flasks were filled with 150 mL of the respective *Synechocystis* culture at stationary phase or with fresh BG-11 culture medium. The flasks were kept shaking for 4 d in the same light intensity the cultures grew in before. After 4 d of culture, the cellular density in the tubes was determined.

Experimental Protocols to Evaluate the Effect of Cell Density on Growth

To investigate whether a cell-cell interaction can negatively affect the growth rate of *Synechocystis* and how the effect is related quantitatively to the cell density of the culture, three different experiments were performed. All the experiments were performed with cultures on urea under 200 μmol photons m^{-2} s^{-1}, where maximum growth rates were achieved.

In the first experiment, the growth cycle of *Synechocystis* was evaluated in cultures starting with four different initial cell densities: 2×10^6, 4×10^6, 6×10^6, and 2×10^7 cells mL^{-1}. The growth cycle and Gt of each treatment were evaluated as described before.

In the second experiment, cell density was artificially increased by 10 times during log phase. For that, cultures of 150 mL were grown until a density of 1×10^7 cells mL^{-1} was reached. They were then separated into three groups: (1) cultures were used as controls (i.e. they were maintained growing); (2) cultures were centrifuged and concentrated 10 times to a final density of 1×10^8 cells mL^{-1}; and (3) cultures were submitted to the same pipetting and centrifugation steps as in group 2 but resuspended without being concentrated (centrifuged controls). The growth of the three groups was then monitored daily as described above.

In the third experiment, *Synechocystis* was grown under fed-batch conditions to evaluate how its growth responds to different dilution rates and cell densities. First, cultures were grown as batch, to assess if their growth properties in a photoreactor were similar to those observed previously in conical flasks. Once cultures reached stationary phase with a similar growth cycle to that used previously, cultures were diluted at a density of 4×10^6 cells mL^{-1}. The medium feed pump was started after 24 h, and the medium was fed at a rate of 5.6 mL medium per hour. This was carried out only during the 180 h of the light period, which meant a daily volume of 100 mL of medium and a daily dilution rate of 0.5×, as the initial volume of culture in the photoreactor was 200 mL. Every day at the beginning of the light period, the volume of the cultures was readjusted to the initial volume of 200 mL. A second daily dilution rate of 2× also was tested by adding 33.4 mL of medium per hour during the light period. Both dilution experiments were also performed with cultures at stationary phase (2×10^8 cells mL^{-1}).

Biomass, Photosynthesis, Metabolic Profile, and Gene Expression Determination

All the physiological, metabolic, and molecular analyses were performed with samples harvested at day 4 (log phase) and 3 d after the onset of the stationary phase, both at ED and EN.

Dry Biomass

Biomass was determined by filtering 50 mL of cultures on nitrocellulose membranes, which had been weighed previously. The material was dried at 70°C for 48 h and then maintained for 24 h in a desiccation chamber with blue silica gel. The weight of the membrane plus biomass was then determined, and the dry biomass weight was obtained by subtraction of the membrane weight.

Oxygen Evolution Analysis

Photosynthesis was analyzed using noninvasive optical oxygen sensors (PreSens). Oxygen sensor spots were glued inside the conical flasks (500 mL) so that they were in contact with the culture. The instrument was calibrated using a solution of sodium hydrosulfite to set 0% saturation and after with distilled water. Analysis was started at the end of the dark period, and after obtaining a stable readout of oxygen levels, the light was switched on. Oxygen evolution was then measured for at least 10 min.

Determination of Metabolite Contents

Samples were collected with a syringe filled with a quenching solution (60% [v/v] methanol in water) precooled to less than −20°C. The solutions were then transferred quickly to centrifuge tubes stored in an ice bath. Each quenched sample was centrifuged for 20 min at 4,000 rpm (Young et al., 2011). Pellets were subjected to hot ethanol extraction (Cross et al., 2006). The soluble fraction was used for the determination of chlorophyll *a* (Ritchie, 2006) and total amino acid contents (Schippers et al., 2008). In the insoluble fraction, protein and glycogen contents were determined according to Lowry et al. (1951) and Hendriks et al. (2003), respectively. Total soluble sugars were determined as described previously (Dubois et al., 1956). The determination of a large set of primary

Downloaded from on August 30, 2017 - Published by www.plantphysiol.org
Copyright © 2017 American Society of Plant Biologists. All rights reserved.

metabolites was performed by gas chromatography coupled with mass spectrometry (GC-MS; Krall et al., 2009), using palatinose as an internal standard. For cyanophycin and phycocyanin determination, samples were sonicated (40% amplitude for 4 min) and subsequently centrifuged for 40 min at 4,000 rpm. Phycocyanin was determined from the supernatant (Tandeau de Marsac, 1977), and cyanophycin was extracted from the remaining pellet as described previously (Burnat et al., 2014) and determined by Sakaguchi reaction (Messineo, 1966).

Gene Expression Analysis

RNA was extracted according to Kim et al. (2006), applying the freeze-thaw step described by Kim et al. (2012) before disrupting the cells in a Tissuelyser (Qiagen). RNA concentration was quantified spectrophotometrically at 260 nm, and its integrity was checked by electrophoresis on a denaturing agarose gel (1.6% [m/v]; Goda and Minton, 1995). Due to the presence of DNA, samples were treated with RNase-free DNase I (Sigma) according to the manufacturer's instructions. For cDNA synthesis 1,000 ng of total RNA was reverse transcribed with the SensiFAST cDNA Synthesis Kit (Bioline) in a final volume of 20 μL, following the manufacturer's instructions. Subsequently, cDNA was diluted three times and stored at −20°C. RT-qPCR was performed on 96-well PCR plates covered with a sealing tape (Thermo), using SensiMix SYBR No-ROX Kit (Bioline), following the manufacturer's instructions. To calculate the relative expression levels of *ntcA*, *pII*, and *ftsZ*, *rnpB* (RNA subunit of RNase P) was selected as the reference gene, as described previously (Pinto et al., 2012).

Experimental Design and Statistical Analysis

The experiments were performed and analyzed according to a randomized block design with three replications. The data obtained at ED and EN were subjected to Student's *t* test at 5% probability. ANOVA ($P < 0.05$) was performed to compare the data obtained for the different growth conditions, and the means were compared by Tukey's test at 5% probability, using the lowest value as a reference. All these analyses were performed with the software package SPSS 22 Windows & Macintosh (Armonk). Finally, the results obtained were analyzed independently via Spearman's correlation using Excel 2013 (Microsoft).

Supplemental Data

The following supplemental materials are available.

Supplemental Figure S1. Relative expression levels of *ftsZ* at ED and EN on the 4th day of culture and 3 d after the onset of the stationary phase.

Supplemental Figure S2. Chlorophyll *a* and phycocyanin levels determined on the 4th day of culture.

Supplemental Figure S3. Total soluble sugars, glycogen, total soluble amino acids, proteins, and cyanophycin levels determined on the 4th day of culture at ED and EN.

Supplemental Figure S4. Total soluble sugar concentrations in the growth medium after 4 d of culture in samples harvested at EN.

Supplemental Figure S5. Percentage of glycogen degraded during the night of the 4th day of culture.

Supplemental Figure S6. Relative expression levels of *ntcA* and *pII* at ED and EN of the 4th day of culture.

Supplemental Figure S7. Chlorophyll *a* and phycocyanin levels 3 d after the onset of stationary phase.

Supplemental Figure S8. Total soluble sugars, Suc, and glycogen levels 3 d after the onset of stationary phase.

Supplemental Figure S9. Total soluble sugar concentrations in the growth medium 3 d after the onset of stationary phase.

Supplemental Figure S10. Total soluble amino acids, Glu, cyanophycin, and protein contents in cells 3 d after the onset of the stationary phase.

Supplemental Figure S11. Spearman's rank coefficient of correlation between all growth, physiological, metabolic, and molecular traits determined at ED and EN on the 4th day of culture.

Supplemental Figure S12. Spearman's rank coefficient of correlation between all growth, physiological, and metabolic traits determined at ED and EN in cells 3 d after the onset of the stationary phase.

Supplemental Figure S13. Glc tolerance test with *Synechocystis* sp. PCC 6803 cultured in mixotrophic conditions in liquid and agar BG11 supplemented with nitrate and different Glc concentrations.

Supplemental Table S1. Cell number after 4 d of culture (log phase) and 3 d after the onset of the stationary phase.

Supplemental Table S2. Cell size in log and stationary phases.

Supplemental Table S3. Cellular dry weight in log and stationary phases.

Supplemental Table S4. Primary metabolites determined by GC-MS at ED on the 4th day of culture.

Supplemental Table S5. Primary metabolites determined by GC-MS at EN on the 4th day of culture.

Supplemental Table S6. Primary metabolites determined by GC-MS at ED of the 3rd day after the onset of stationary phase.

Supplemental Table S7. Primary metabolites determined by GC-MS at EN of the 3rd day after the onset of stationary phase.

Supplemental Table S8. Cell density of an inoculum grown on filtered medium from a previous culture that had reached stationary phase or whole cell culture that had reached stationary phase and was regrown without dilution on fresh medium.

Supplemental Table S9. Cell density of an inoculum grown on filtered medium from a previous culture that had reached stationary phase or whole cell culture that had reached stationary phase and was regrown without dilution on fresh medium.

Received May 31, 2017; accepted June 20, 2017; published June 23, 2017.

LITERATURE CITED

Agostoni M, Waters CM, Montgomery BL (2016) Regulation of biofilm formation and cellular buoyancy through modulating intracellular cyclic di-GMP levels in engineered cyanobacteria. Biotechnol Bioeng **113:** 311–319

Alfonso M, Perewoska I, Kirilovsky D (2000) Redox control of *psb*A gene expression in the cyanobacterium *Synechocystis* PCC 6803: involvement of the cytochrome b_6/f complex. Plant Physiol **122:** 505–516

Alfonso M, Perewoska I, Kirilovsky D (2001) Redox control of *ntc*A gene expression in *Synechocystis* sp. PCC 6803: nitrogen availability and electron transport regulate the levels of the NtcA protein. Plant Physiol **125:** 969–981

Arteni AA, Ajlani G, Boekema EJ (2009) Structural organisation of phycobilisomes from *Synechocystis* sp. strain PCC6803 and their interaction with the membrane. Biochim Biophys Acta **1787:** 272–279

Badger MR, Price GD, Long BM, Woodger FJ (2006) The environmental plasticity and ecological genomics of the cyanobacterial CO_2 concentrating mechanism. J Exp Bot **57:** 249–265

Baebprasert W, Jantaro S, Khetkorn W, Lindblad P, Incharoensakdi A (2011) Increased H_2 production in the cyanobacterium *Synechocystis* sp. strain PCC 6803 by redirecting the electron supply via genetic engineering of the nitrate assimilation pathway. Metab Eng **13:** 610–616

Beck C, Knoop H, Axmann IM, Steuer R (2012) The diversity of cyanobacterial metabolism: genome analysis of multiple phototrophic microorganisms. BMC Genomics **13:** 56

Belas R (2014) Biofilms, flagella, and mechanosensing of surfaces by bacteria. Trends Microbiol **22:** 517–527

Berla BM, Pakrasi HB (2012) Upregulation of plasmid genes during stationary phase in *Synechocystis* sp. strain PCC 6803, a cyanobacterium. Appl Environ Microbiol **78:** 5448–5451

Brennan L, Owende P (2010) Biofuels from microalgae: a review of technologies for production, processing, and extractions of biofuels and co-products. Renew Sustain Energy Rev **14:** 557–577

Brown AD (1976) Microbial water stress. Bacteriol Rev **40:** 803–846

Burnap RL (2015) Systems and photosystems: cellular limits of autotrophic productivity in cyanobacteria. Front Bioeng Biotechnol **3:** 1–13

Burnat M, Herrero A, Flores E (2014) Compartmentalized cyanophycin metabolism in the diazotrophic filaments of a heterocyst-forming cyanobacterium. Proc Natl Acad Sci USA **111:** 3823–3828

Downloaded from on August 30, 2017 - Published by www.plantphysiol.org
Copyright © 2017 American Society of Plant Biologists. All rights reserved.

Catling DC, Zahnle KJ, McKay C (2001) Biogenic methane, hydrogen escape, and the irreversible oxidation of early Earth. Science **293:** 839–843

Cross JM, von Korff M, Altmann T, Bartzetko L, Sulpice R, Gibon Y, Palacios N, Stitt M (2006) Variation of enzyme activities and metabolite levels in 24 Arabidopsis accessions growing in carbon-limited conditions. Plant Physiol **142:** 1574–1588

Dexter J, Fu P (2009) Metabolic engineering of cyanobacteria for ethanol production. Energy Environ Sci **2:** 857–864

Dubois M, Gilles KA, Hamilton JK, Rebers PA, Smith F (1956) Colorimetric method for determination of sugars and related substances. Anal Chem **28:** 350–356

Ellison C, Brun YV (2015) Mechanosensing: a regulation sensation. Curr Biol **25:** R113–R115

Espinosa J, Rodríguez-Mateos F, Salinas P, Lanza VF, Dixon R, de la Cruz F, Contreras A (2014) PipX, the coactivator of NtcA, is a global regulator in cyanobacteria. Proc Natl Acad Sci USA **111:** E2423–E2430

Flores E, Frías JE, Rubio LM, Herrero A (2005) Photosynthetic nitrate assimilation in cyanobacteria. Photosynth Res **83:** 117–133

Flores E, Herrero A (2005) Nitrogen assimilation and nitrogen control in cyanobacteria. Biochem Soc Trans **33:** 164–167

Frommeyer M, Wiefel L, Steinbüchel A (2016) Features of the biotechnologically relevant polyamide family "cyanophycins" and their biosynthesis in prokaryotes and eukaryotes. Crit Rev Biotechnol **36:** 153–164

García-Domínguez M, Florencio FJ (1997) Nitrogen availability and electron transport control the expression of *gln*B gene (encoding PII protein) in the cyanobacterium *Synechocystis* sp. PCC 6803. Plant Mol Biol **35:** 723–734

Goda SK, Minton NP (1995) A simple procedure for gel electrophoresis and northern blotting of RNA. Nucleic Acids Res **23:** 3357–3358

Hagemann M (2011) Molecular biology of cyanobacterial salt acclimation. FEMS Microbiol Rev **35:** 87–123

Hagemann M, Kern R, Maurino VG, Hanson DT, Weber APM, Sage RF, Bauwe H (2016) Evolution of photorespiration from cyanobacteria to land plants, considering protein phylogenies and acquisition of carbon concentrating mechanisms. J Exp Bot **67:** 2963–2976

He X, Ahn J (2011) Differential gene expression in planktonic and biofilm cells of multiple antibiotic-resistant *Salmonella typhimurium* and *Staphylococcus aureus*. FEMS Microbiol Lett **325:** 180–188

Hendriks JHM, Kolbe A, Gibon Y, Stitt M, Geigenberger P (2003) ADP-glucose pyrophosphorylase is activated by posttranslational redox-modification in response to light and to sugars in leaves of Arabidopsis and other plant species. Plant Physiol **133:** 838–849

Herrero A, Muro-Pastor AM, Flores E (2001) Nitrogen control in cyanobacteria. J Bacteriol **183:** 411–425

Hihara Y, Kamei A, Kanehisa M, Kaplan A, Ikeuchi M (2001) DNA microarray analysis of cyanobacterial gene expression during acclimation to high light. Plant Cell **13:** 793–806

Iijima H, Nakaya Y, Kuwahara A, Hirai MY, Osanai T (2015) Seawater cultivation of freshwater cyanobacterium *Synechocystis* sp. PCC 6803 drastically alters amino acid composition and glycogen metabolism. Front Microbiol **6:** 326

Imanaka H, Tanaka S, Feng B, Imamura K, Nakanishi K (2010) Cultivation characteristics and gene expression profiles of *Aspergillus oryzae* by membrane-surface liquid culture, shaking-flask culture, and agar-plate culture. J Biosci Bioeng **109:** 267–273

Joseph A, Aikawa S, Sasaki K, Matsuda F, Hasunuma T, Kondo A (2014) Increased biomass production and glycogen accumulation in *apc*E gene deleted *Synechocystis* sp. PCC 6803. AMB Express **4:** 17

Kanesaki Y, Shiwa Y, Tajima N, Suzuki M, Watanabe S, Sato N, Ikeuchi M, Yoshikawa H (2012) Identification of substrain-specific mutations by massively parallel whole-genome resequencing of *Synechocystis* sp. PCC 6803. DNA Res **19:** 67–79

Kasting JF, Siefert JL (2002) Life and the evolution of Earth's atmosphere. Science **296:** 1066–1068

Kim BH, Oh HM, Lee YK, Choi GG, Ahn CY, Yoon BD, Kim HS (2006) Simple method for RNA preparation from cyanobacteria. J Phycol **42:** 1137–1141

Kim BH, Ramanan R, Cho DH, Choi GG, La HJ, Ahn CY, Oh HM, Kim HS (2012) Simple, rapid and cost-effective method for high quality nucleic acids extraction from different strains of *Botryococcus braunii*. PLoS ONE **7:** e37770

Kim HW, Vannela R, Zhou C, Rittmann BE (2011) Nutrient acquisition and limitation for the photoautotrophic growth of *Synechocystis* sp. PCC6803 as a renewable biomass source. Biotechnol Bioeng **108:** 277–285

Kopecná J, Komenda J, Bucinská L, Sobotka R (2012) Long-term acclimation of the cyanobacterium *Synechocystis* sp. PCC 6803 to high light is accompanied by an enhanced production of chlorophyll that is preferentially channeled to trimeric photosystem I. Plant Physiol **160:** 2239–2250

Krall L, Huege J, Catchpole G, Steinhauser D, Willmitzer L (2009) Assessment of sampling strategies for gas chromatography-mass spectrometry (GC-MS) based metabolomics of cyanobacteria. J Chromatogr B Analyt Technol Biomed Life Sci **877:** 2952–2960

Kühl M, Chen M, Ralph PJ, Schreiber U, Larkum AWD (2005) Ecology: a niche for cyanobacteria containing chlorophyll d. Nature **433:** 820

Lamb JJ, Hill RE, Eaton-Rye JJ, Hohmann-Marriott MF (2014) Functional role of PilA in iron acquisition in the cyanobacterium *Synechocystis* sp. PCC 6803. PLoS ONE **9:** e105761

Law AE, Mullineaux CW, Hirst EM, Saldanha J, Wilson RJ (2000) Bacterial orthologues indicate the malarial plastid gene *ycf*24 is essential. Protist **151:** 317–327

Lazazzera BA (2000) Quorum sensing and starvation: signals for entry into stationary phase. Curr Opin Microbiol **3:** 177–182

Lea-Smith DJ, Bombelli P, Dennis JS, Scott SA, Smith AG, Howe CJ (2014) Phycobilisome-deficient strains of *Synechocystis* sp. PCC 6803 have reduced size and require carbon-limiting conditions to exhibit enhanced productivity. Plant Physiol **165:** 705–714

Lee HM, Vázquez-Bermúdez MF, de Marsac NT (1999) The global nitrogen regulator NtcA regulates transcription of the signal transducer PII (GlnB) and influences its phosphorylation level in response to nitrogen and carbon supplies in the cyanobacterium *Synechococcus* sp. strain PCC 7942. J Bacteriol **181:** 2697–2702

Liu H, Zhang H, Niedzwiedzki DM, Prado M, He G, Gross ML, Blankenship RE (2013) Phycobilisomes supply excitations to both photosystems in a megacomplex in cyanobacteria. Science **342:** 1104–1107

Liu X, Sheng J, Curtiss R III (2011) Fatty acid production in genetically modified cyanobacteria. Proc Natl Acad Sci USA **108:** 6899–6904

Llácer JL, Espinosa J, Castells MA, Contreras A, Forchhammer K, Rubio V (2010) Structural basis for the regulation of NtcA-dependent transcription by proteins PipX and PII. Proc Natl Acad Sci USA **107:** 15397–15402

Lowry OH, Rosebrough NJ, Farr AL, Randall RJ (1951) Protein measurement with the Folin phenol reagent. J Biol Chem **193:** 265–275

Lüddecke J, Forchhammer K (2015) Energy sensing versus 2-oxoglutarate dependent ATPase switch in the control of *Synechococcus* PII interaction with its targets NAGK and PipX. PLoS ONE **10:** e0137114

Mackay MA, Norton RS, Borowitzka LJ (1984) Organic osmoregulatory solutes in cyanobacteria. Microbiology **130:** 2177–2191

Markou G, Georgakakis D (2011) Cultivation of filamentous cyanobacteria (blue-green algae) in agro-industrial wastes and wastewaters: a review. Appl Energy **88:** 3389–3401

Messineo L (1966) Modification of the Sakaguchi reaction: spectrophotometric determination of arginine in proteins without previous hydrolysis. Arch Biochem Biophys **117:** 534–540

Miao X, Wu Q, Wu G, Zhao N (2003) Sucrose accumulation in salt-stressed cells of agp gene deletion-mutant in cyanobacterium Synechocystis sp PCC 6803. FEMS Microbiol Lett **218:** 71–77

Mikkat S, Effmert U, Hagemann M (1997) Uptake and use of the osmoprotective compounds trehalose, glucosylglycerol, and sucrose by the cyanobacterium *Synechocystis* sp. PCC 6803. Arch Microbiol **167:** 112–118

Mori T, Johnson CH (2001) Independence of circadian timing from cell division in cyanobacteria. J Bacteriol **183:** 2439–2444

Mullineaux CW (2008) Phycobilisome-reaction centre interaction in cyanobacteria. Photosynth Res **95:** 175–182

Muramatsu M, Hihara Y (2012) Acclimation to high-light conditions in cyanobacteria: from gene expression to physiological responses. J Plant Res **125:** 11–39

Muramatsu M, Sonoike K, Hihara Y (2009) Mechanism of downregulation of photosystem I content under high-light conditions in the cyanobacterium *Synechocystis* sp. PCC 6803. Microbiology **155:** 989–996

Muro-Pastor MI, Reyes JC, Florencio FJ (2005) Ammonium assimilation in cyanobacteria. Photosynth Res **83:** 135–150

Downloaded from on August 30, 2017 - Published by www.plantphysiol.org
Copyright © 2017 American Society of Plant Biologists. All rights reserved.

Nakasugi K, Neilan BA (2005) Identification of pilus-like structures and genes in *Microcystis aeruginosa* PCC7806. Appl Environ Microbiol **71:** 7621–7625

Ort DR, Melis A (2011) Optimizing antenna size to maximize photosynthetic efficiency. Plant Physiol **155:** 79–85

Oswald O, Martin T, Dominy PJ, Graham IA (2001) Plastid redox state and sugars: interactive regulators of nuclear-encoded photosynthetic gene expression. Proc Natl Acad Sci USA **98:** 2047–2052

Parnasa R, Nagar E, Sendersky E, Reich Z, Simkovsky R, Golden S, Schwarz R (2016) Small secreted proteins enable biofilm development in the cyanobacterium *Synechococcus elongatus*. Sci Rep **6:** 32209

Pinto F, Pacheco CC, Ferreira D, Moradas-Ferreira P, Tamagnini P (2012) Selection of suitable reference genes for RT-qPCR analyses in cyanobacteria. PLoS ONE **7:** e34983

Price GD, Sültemeyer D, Klughammer B, Ludwig M, Badger MR (1998) The functioning of the CO_2 concentrating mechanism in several cyanobacterial strains: a review of general physiological characteristics, genes, proteins, and recent advances. Can J Bot **76:** 973–1002

Quintero MJ, Muro-Pastor AM, Herrero A, Flores E (2000) Arginine catabolism in the cyanobacterium *Synechocystis* sp. strain PCC 6803 involves the urea cycle and arginase pathway. J Bacteriol **182:** 1008–1015

Raven JA, Kübler JE (2002) New light on the scaling of metabolic rate with the size of algae. J Phycol **38:** 11–16

Rippka R, Deruelles J, Waterbury JB, Herdman M, Stanier RY (1979) Generic assignments, strain histories and properties of pure cultures of cyanobacteria. J Gen Microbiol **111:** 1–61

Ritchie RJ (2006) Consistent sets of spectrophotometric chlorophyll equations for acetone, methanol and ethanol solvents. Photosynth Res **89:** 27–41

Romero-Lastra P, Sánchez MC, Ribeiro-Vidal H, Llama-Palacios A, Figuero E, Herrera D, Sanz M (2017) Comparative gene expression analysis of *Porphyromonas gingivalis* ATCC 33277 in planktonic and biofilms states. PLoS ONE **12:** e0174669

Schatz D, Nagar E, Sendersky E, Parnasa R, Zilberman S, Carmeli S, Mastai Y, Shimoni E, Klein E, Yeger O, et al (2013) Self-suppression of biofilm formation in the cyanobacterium *Synechococcus elongatus*. Environ Microbiol **15:** 1786–1794

Schenk PM, Thomas-Hall SR, Stephens E, Marx UC, Mussgnug JH, Posten C, Kruse O, Hankamer B (2008) Second generation biofuels: high-efficiency microalgae for biodiesel production. BioEnergy Res **1:** 20–43

Schippers JHM, Nunes-Nesi A, Apetrei R, Hille J, Fernie AR, Dijkwel PP (2008) The *Arabidopsis* onset of leaf death5 mutation of quinolinate synthase affects nicotinamide adenine dinucleotide biosynthesis and causes early ageing. Plant Cell **20:** 2909–2925

Schirrmeister BE, de Vos JM, Antonelli A, Bagheri HC (2013) Evolution of multicellularity coincided with increased diversification of cyanobacteria and the Great Oxidation Event. Proc Natl Acad Sci USA **110:** 1791–1796

Schuurmans RM, Matthijs JCP, Hellingwerf KJ (2017) Transition from exponential to linear photoautotrophic growth changes the physiology of *Synechocystis* sp. PCC 6803. Photosynth Res **132:** 69–82

Schuurmans RM, van Alphen P, Schuurmans JM, Matthijs HCP, Hellingwerf KJ (2015) Comparison of the photosynthetic yield of cyanobacteria and green algae: different methods give different answers. PLoS ONE **10:** e0139061

Sekar S, Chandramohan M (2008) Phycobiliproteins as a commodity: trends in applied research, patents and commercialization. J Appl Phycol **20:** 113–136

Sharif DI, Gallon J, Smith CJ, Dudley E (2008) Quorum sensing in cyanobacteria:N-octanoyl-homoserine lactone release and response, by the epilithic colonial cyanobacterium *Gloeothece* PCC6909. ISME J **2:** 1171–1182

Shiloach J, Fass R (2005) Growing *E. coli* to high cell density: a historical perspective on method development. Biotechnol Adv **23:** 345–357

Slade R, Bauen A (2013) Micro-algae cultivation for biofuels: cost, energy balance, environmental impacts and future prospects. Biomass Bioenergy **53:** 29–38

Stitt M, von Schaewen A, Willmitzer L (1991) "Sink" regulation of photosynthetic metabolism in transgenic tobacco plants expressing yeast invertase in their cell wall involves a decrease of the Calvin-cycle enzymes and an increase of glycolytic enzymes. Planta **183:** 40–50

Tandeau de Marsac N (1977) Occurrence and nature of chromatic adaptation in cyanobacteria. J Bacteriol **130:** 82–91

Tomitani A, Knoll AH, Cavanaugh CM, Ohno T (2006) The evolutionary diversification of cyanobacteria: molecular-phylogenetic and paleontological perspectives. Proc Natl Acad Sci USA **103:** 5442–5447

Touloupakis E, Cicchi B, Torzillo G (2015) A bioenergetic assessment of photosynthetic growth of *Synechocystis* sp. PCC 6803 in continuous cultures. Biotechnol Biofuels **8:** 133

Valladares A, Montesinos ML, Herrero A, Flores E (2002) An ABC-type, high-affinity urea permease identified in cyanobacteria. Mol Microbiol **43:** 703–715

van Alphen P, Hellingwerf KJ (2015) Sustained circadian rhythms in continuous light in *Synechocystis* sp. PCC6803 growing in a well-controlled photobioreactor. PLoS ONE **10:** e0127715

Wijffels RH, Kruse O, Hellingwerf KJ (2013) Potential of industrial biotechnology with cyanobacteria and eukaryotic microalgae. Curr Opin Biotechnol **24:** 405–413

Williams JGK (1988) Construction of specific mutations in photosystem II photosynthetic reaction center by genetic engineering methods in Synechocystis 6803. Methods Enzymol **167:** 766–778

Yang Q, Pando BF, Dong G, Golden SS, van Oudenaarden A (2010) Circadian gating of the cell cycle revealed in single cyanobacterial cells. Science **327:** 1522–1526

Young JD, Shastri AA, Stephanopoulos G, Morgan JA (2011) Mapping photoautotrophic metabolism with isotopically nonstationary ^{13}C flux analysis. Metab Eng **13:** 656–665

Yu Y, You L, Liu D, Hollinshead W, Tang YJ, Zhang F (2013) Development of Synechocystis sp. PCC 6803 as a phototrophic cell factory. Mar Drugs **11:** 2894–2916

Zavřel T, Sinetova MA, Búzová D, Literáková P, Červený J (2015) Characterization of a model cyanobacterium *Synechocystis* sp. PCC 6803 autotrophic growth in a flat-panel photobioreactor. Eng Life Sci **15:** 122–132

Zhao MX, Jiang YL, He YX, Chen YF, Teng YB, Chen Y, Zhang CC, Zhou CZ (2010) Structural basis for the allosteric control of the global transcription factor NtcA by the nitrogen starvation signal 2-oxoglutarate. Proc Natl Acad Sci USA **107:** 12487–12492

Downloaded from on August 30, 2017 - Published by www.plantphysiol.org
Copyright © 2017 American Society of Plant Biologists. All rights reserved.